

Partial wave analysis of η photoproduction data

M. Hadzimehmedovic, R. Omerovic, H. Osmanovic and
J. Stahov for Mainz, Tuzla, Zagreb collaboration (**MTZ**)

University of Tuzla, Faculty of Science, Bosnia and Herzegovina

Mainz, February 15, 2016



- Single energy partial wave analysis - SE PWA-generally
- Imposing the fixed-t analyticity in PWA-generally
- Preliminary results
- Problem: Dependence on constraining PW solution
- Search for unique solution
- Conclusions
- Further research



Single energy partial wave analysis

At a given energy W minimize a quadratic form:

$$\chi_{data}^2 = \sum_D \sum_{k=1}^{N_D} \left(\frac{D_k^{exp}(\theta_k) - D_k^{fit}(\theta_k)}{\Delta_{D_k}} \right)^2$$

$D_k^{exp}(\theta_k)$ – values of observable D measured at angles θ_k with errors Δ_{D_k} .

$D_k^{fit}(\theta_k)$ - predictions calculated from partial waves (multipoles) which are parameters in the fit.

Serious problem in SE PWA - ambiguities, no unique solution.

How to resolve it?

First attempt:

Require smoothness of partial waves as a function of energy -

without success.



One must impose more stringent constraints taking into account analyticity of scattering amplitudes.

(J. S. Bowcock, H. Burkhardt, Rep. Prog Phys 38 (1975) 1099)

Important step forward:

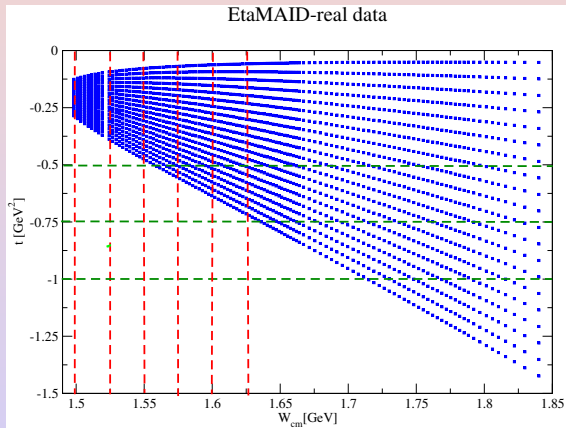
- E. Pietarinen: Amplitude analysis using fixed-t analyticity of invariant amplitudes
 - E. Pietarinen, Nuovo Cim. 12 (1972) 522
 - E. Pietarinen, Nucl. Phys. B49 (1972) 315 Discussion of uniqueness problem
 - E. Pietarinen, Nucl. Phys. 8107 (1976) 21 Discussion of uniqueness problem
 - J. Hamilton, J. L. Peterson, New developments in dispersion theory, Vol.1, Nordita, 1975.



- The method consists of two separated analysis:
 - Fixed-t amplitude analysis - a method which can determine the scattering amplitudes from exp. data at fixed-t
 - Single energy partial wave analysis - SE PWA
- Fixed-t AA and SE PWA are coupled. Results from one analysis are used as constraint in another in an iterative procedure.
- Method was used in famous KH80 analysis of πN scattering data.
- In Mainz-Tuzla-Zagreb PWA of η - photoproduction data we apply the same principles.



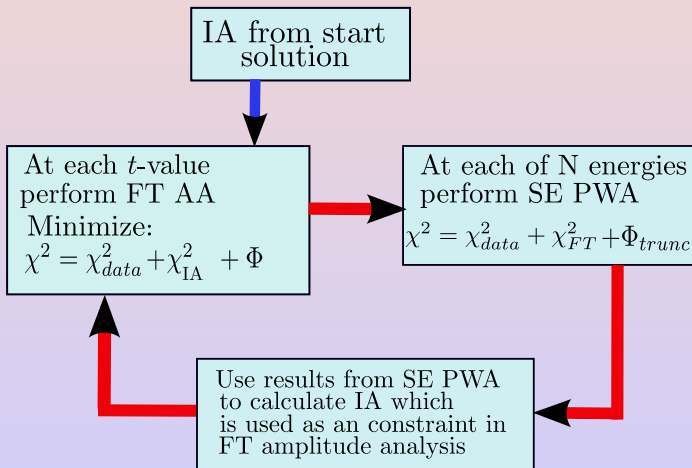
Imposing the fixed-t analyticity in PWA of scattering data



Red dashed lines-SE PWA, Green dashed lines - fixed-t amplitude analysis



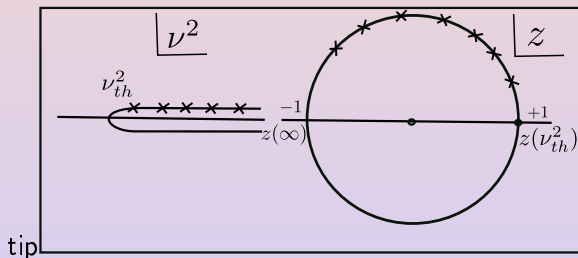
Imposing the fixed- t analyticity in PWA of scattering data



Pietarinen's expansion method

The simplest case- πN elastic scattering at fixed- t .

Apart from nucleon poles, crossing symmetric invariant amplitudes are analytic function in a complex ν^2 plane $\nu_{th}^2 \leq \nu^2 < \infty$, ($\nu_{th} = m_\pi + \frac{t}{4m}$).



Conformal mapping:

$$z = \frac{\alpha - \sqrt{\nu_{th}^2 - \nu^2}}{\alpha + \sqrt{\nu_{th}^2 - \nu^2}}$$

maps a cut ν^2 plane inside and on the circle in a z plane.

Pietarinen expansion method: Invariant amplitudes C^\pm , B^\pm represented by:

$$C^\pm(\nu^2, t) = C_N^\pm(\nu^2, t) + \hat{C}^\pm(\nu^2, t) \sum_{n=0}^{\infty} c_n^\pm z^n$$

$$B^\pm(\nu^2, t) = B_N^\pm(\nu^2, t) + \hat{B}^\pm(\nu^2, t) \sum_{n=0}^{\infty} b_n^\pm z^\pm$$

C_N^\pm , B_N^\pm - nucleon pole contributions, $\hat{C}^\pm(\nu^2, t)$, $\hat{B}^\pm(\nu^2, t)$ describe high energy behaviour of IA.



Pietarinen's expansion method

Pietarinen: The best approximants of IA are to be determined by minimizing a quadratic form:

$$\chi^2 = \chi_{data}^2 + \Phi.$$

Φ is a convergence test function:

$$\Phi = \lambda_1 \Phi_1 + \lambda_2 \Phi_2 + \lambda_3 \Phi_3 + \lambda_4 \Phi_4.$$

$$\Phi_1 = \sum_{n=0}^N (n+1)^3 (c_n^+)^2, \dots, \Phi_4 = \sum_{n=0}^N (n+1)^3 (b_n^-)^2.$$

For $N \approx 30$:

$$\lambda_1 = \frac{N}{\sum_{n=0}^N (n+1)^3 (c_n^+)^2}, \dots, \lambda_4 = \frac{N}{\sum_{n=0}^N (n+1)^3 (b_n^-)^2}.$$



Our PWA of η photoproduction data consists of two analysis:

- Fixed-t amplitude analysis
- SE PWA

Fixed- t amplitude analysis requires experimental data at a given value of variable t. Experimental data have to be shifted to predefined t-values using a small steps in t - **t-binning**.

SE PWA requires experimental data at a given energy.

Experimental data have to be shifted to predefined energies-**energy binning**.



Fixed-t amplitude analysis

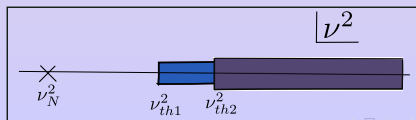
For a given t crossing symmetric invariant amplitudes are represented by two Pietarinen series:

$$B_1 = B_{1N} + \sum_{i=0}^{N_1} b_{1i}^{(1)} z_1^i + \sum_{i=0}^{N_2} b_{1i}^{(2)} z_2^i, \quad B_2 = B_{2N} + \sum_{i=0}^{N_1} b_{2i}^{(1)} z_1^i + \sum_{i=0}^{N_2} b_{2i}^{(2)} z_2^i$$

$$B_6 = B_{6N} + \sum_{i=0}^{N_1} b_{6i}^{(1)} z_1^i + \sum_{i=0}^{N_2} b_{6i}^{(2)} z_2^i, \quad B_8 = \frac{B_{8N}}{\nu} + \sum_{i=0}^{N_1} b_{8i}^{(1)} z_1^i + \sum_{i=0}^{N_2} b_{8i}^{(2)} z_2^i$$

B_{iN} are known nucleon pole contributions. Conformal variables z_1 and z_2 are defined as:

$$z_1 = \frac{\alpha - \sqrt{\nu_{th1}^2 - \nu^2}}{\alpha + \sqrt{\nu_{th1}^2 - \nu^2}}, \quad z_2 = \frac{\beta - \sqrt{\nu_{th2}^2 - \nu^2}}{\beta + \sqrt{\nu_{th2}^2 - \nu^2}}.$$



Fixed-t amplitude analysis

Coefficients $\{b_1^{(k)}\}$ and $\{b_2^{(k)}\}$ are obtained by minimizing a quadratic form

$$\chi^2 = \chi_{data}^2 + \chi_{PW}^2 + \Phi$$

$$\begin{aligned}\chi_{data}^2 &= \sum_{i=1}^{N^E} \left(\frac{\frac{d\sigma}{d\Omega}(W_i)^{exp} - \frac{d\sigma}{d\Omega}(W_i)^{fit}}{\Delta \frac{d\sigma}{d\Omega}(W_i)^{exp}} \right)^2 \\ &+ \sum_{i=1}^{N^E} \left(\frac{T(W_i)^{exp} - T(W_i)^{fit}}{\Delta T(W_i)^{exp}} \right)^2 \\ &+ \sum_{i=1}^{N^E} \left(\frac{F(W_i)^{exp} - F(W_i)^{fit}}{\Delta F(W_i)^{exp}} \right)^2 \\ &+ \sum_{i=1}^{N^E} \left(\frac{\Sigma(W_i)^{exp} - \Sigma(W_i)^{fit}}{\Delta \Sigma(W_i)^{exp}} \right)^2\end{aligned}$$



Fixed-t amplitude analysis

χ_{PW}^2 contains as a “data” the helicity amplitudes calculated from partial wave solution:

$$\chi_{PW}^2 = q \sum_{i=1}^{N^E} \left(\frac{\text{Re } H_k(W_i)^{PW} - \text{Re } H_k(W_i)^{fit}}{(\varepsilon_R)_{ki}} \right)^2 + q \sum_{k=1}^4 \sum_{i=1}^{N^E} \left(\frac{\text{Im } H_k(W_i)^{PW} - \text{Im } H_k(W_i)^{fit}}{(\varepsilon_I)_{ki}} \right)^2$$

q - adjustable weight factor

Errors ε_{Rk} and ε_{Ik} are adjusted in such a way to get $\chi_{data}^2 \approx \chi_{PW}^2$.

In a first iteration amplitudes H_k^{PW} are calculated from initial, already existing PW solution.

In subsequent iterations H_k^{PW} are calculated from multipoles obtained in SE PWA of the same set of experimental data.



Φ is Pietarinen's convergence test function

$$\Phi = \Phi_1 + \Phi_2 + \Phi_3 + \Phi_4$$

$$\Phi_k = \lambda_{1k} \sum_{i=0}^{N_1} (b_{1i}^{(k)})^2 (n+1)^3 + \lambda_{2k} \sum_{i=0}^{N_2} (b_{2i}^{(k)})^2 (i+1)^3$$

$$\lambda_{1k} = \frac{N_1}{\sum_{i=0}^{N_1} (b_{1i}^{(k)})^2 (i+1)^3}, \quad \lambda_{2k} = \frac{N_2}{\sum_{i=0}^{N_2} (b_{2i}^{(k)})^2 (i+1)^3}$$

One starts with some initial values of coefficients $\{b_1^{(k)}\}$, $\{b_2^{(k)}\}$ and determines λ_{1k} and λ_{2k} in an iterative procedure.



Conection between fixed-t AA and SE PWA

After performing fixed-t amplitude analysis at predetermined t -values, helicity amplitudes may be calculated at any energy W at N_c values of scattering angle

$$\cos\theta_i = \frac{t_i - m_\eta^2 + 2k\omega}{2kq} \quad |\cos\theta_i| \leq 1, \quad t_i \in [t_{min}, t_{max}]$$

These values of helicity amplitudes are used as constraint in SE PWA.



In a single energy partial wave analysis we minimize a quadratic form:

$$\chi^2 = \chi_{data}^2 + \chi_{FT}^2 + \Phi_{trunc}$$

χ_{data}^2 contains all experimental data at a given energy W :

$$\begin{aligned}\chi_{data}^2 &= \sum_{i=1}^{N_1^D} \left(\frac{\frac{d\sigma}{d\Omega}(\theta_i)^{exp} - \frac{d\sigma}{d\Omega}(\theta_i)^{fit}}{\Delta \frac{d\sigma}{d\Omega}(W_i)^{exp}} \right)^2 \\ &+ \sum_{i=1}^{N_2^D} \left(\frac{T(\theta_i)^{exp} - T(\theta_i)^{fit}}{\Delta T(W_i)^{exp}} \right)^2 \\ &+ \sum_{i=1}^{N_3^D} \left(\frac{F(\theta_i)^{exp} - F(\theta_i)^{fit}}{\Delta F(W_i)^{exp}} \right)^2 \\ &+ \sum_{i=1}^{N_4^D} \left(\frac{\Sigma(\theta_i)^{exp} - \Sigma(\theta_i)^{fit}}{\Delta \Sigma(W_i)^{exp}} \right)^2\end{aligned}$$



χ_{FT}^2 contains as the “data” the helicity amplitudes from the fixed-t amplitudes analysis.

$$\chi_{FT}^2 = q \sum_{k=1}^4 \sum_{i=1}^{N^C} \left(\frac{\text{Re } H_k(\theta_i)^{PW} - \text{Re } H_k(\theta_i)^{fit}}{(\varepsilon_R)_{ki}} \right)^2 + q \sum_{k=1}^4 \sum_{i=1}^{N^C} \left(\frac{\text{Im } H_k(\theta_i)^{PW} - \text{Im } H_k(\theta_i)^{fit}}{(\varepsilon_I)_{ki}} \right)^2$$

q - adjustable weight factor

N^C - number of angles at which constraining amplitudes are determined. Errors ε_{Rk} and ε_{Ik} are adjusted in such a way to get $\chi_{data}^2 \approx \chi_{FT}^2$.

Connection between SE PWA and fixed-t AA

Multipoles obtained from SE PWA at N^E energies are used to calculate helicity amplitudes which are used as constraint in the fixed-t amplitude analysis.



$$\Phi_{trunc} = \lambda \sum_{\ell=0}^{\ell_{max}} [|\text{Re} T_{\ell\pm}|^2 R_1^{2\ell} + |\text{Im} T_{\ell\pm}|^2 R_2^{2\ell}]. \quad (1)$$

Expansion in terms of Legendre polynomials converge in an ellipse in $\cos\theta$ plane having $-1, 1$ as foci and semi-axis $y_0(s)$ and $(y_0^2(s) - 1)^{\frac{1}{2}}$, where $y_0(s)$ is determined by the edge of the nearest duple spectral region. In a simplest (spinless) case, pw expansion converges if

$$(\text{Im} T_{\ell})^2 \leq [y_0 + \sqrt{y_0^2 - 1}]^{-2\ell}$$

In a first attempt, we take:

$$R_1 = R_2 = R = x_4 + \sqrt{x_4^2 - 1}$$

when

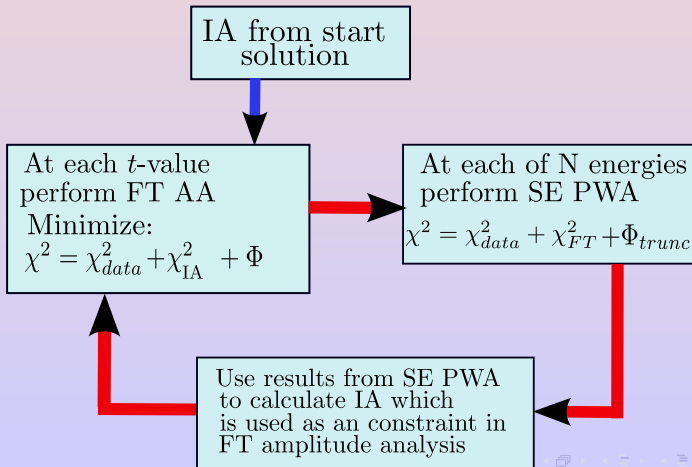
$$y_0 = x_4 = \cos\theta(t = 4m_{\pi}^2)$$

$T_{\ell\pm}$ stands for electric and magnetic multipoles $E_{\ell\pm}$ and $M_{\ell\pm}$.
Makes soft cut off of higher partial waves. Effective at low energies.



Constrained PWA of η photoproduction data

The whole procedure has to be iterated until reaching reasonable agreement in two subsequent iterations



Data base consists of following experimental data

- Differential cross section $\frac{d\sigma}{d\Omega}$
CBall/MAMI: E.McNicoll et al., PRC 82(2010) 035208
 $E_{lab} = 710, \dots, 1395 \text{ MeV}$
2400 data points at 120 energies
- Beam asymmetry Σ
GRAAL: O. Bartalini et al., EPJ A 33 (2007) 169
 $E_{lab} = 724, \dots, 1472 \text{ MeV}$
150 data points at 15 energies
- Target asymmetry T
CBall/MAMI: V. Kashevarov (preliminary)
 $E_{lab} = 725, \dots, 1350 \text{ MeV}$
144 data points at 12 energies
- Double-polarisation asymmetry F
CBall/MAMI: V. Kashevarov (preliminary)
 $E_{lab} = 725, \dots, 1350 \text{ MeV}$
144 data points at 12 energies

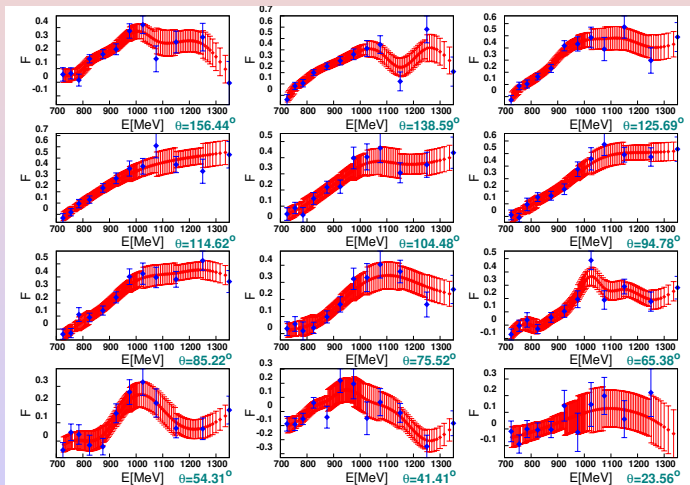


F, T, Σ

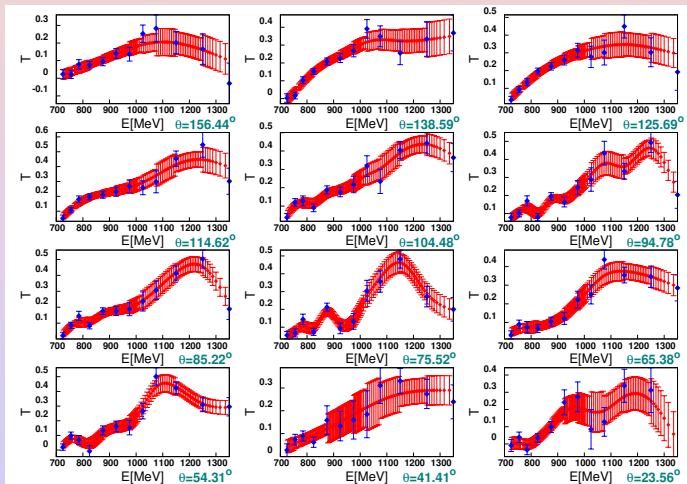
Experimental values of double-polarisation asymmetry F , target asymmetry T , and beam asymmetry Σ for given angles are interpolated to the energies where $\frac{d\sigma}{d\Omega}$ are available. We use a spline fit method. Errors of interpolated data are taken to be equal to errors of nearest measured data points.



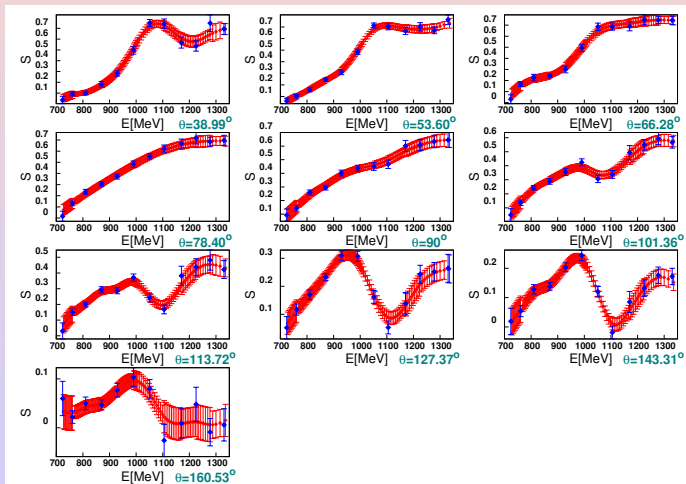
Interpolated values of double polarisation F



Interpolated values of target asymmetry T



Interpolated values of beam asymmetry Σ

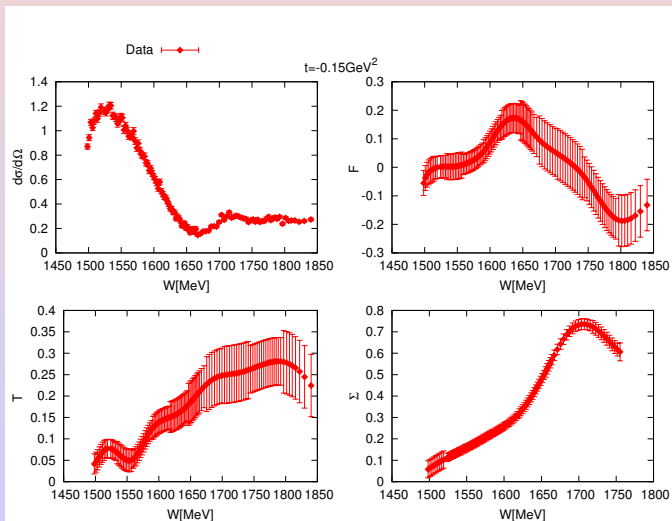


Input data $\frac{d\sigma}{d\Omega}$, T , F and Σ for t-binning are obtained from energy binning procedure (113 energies).

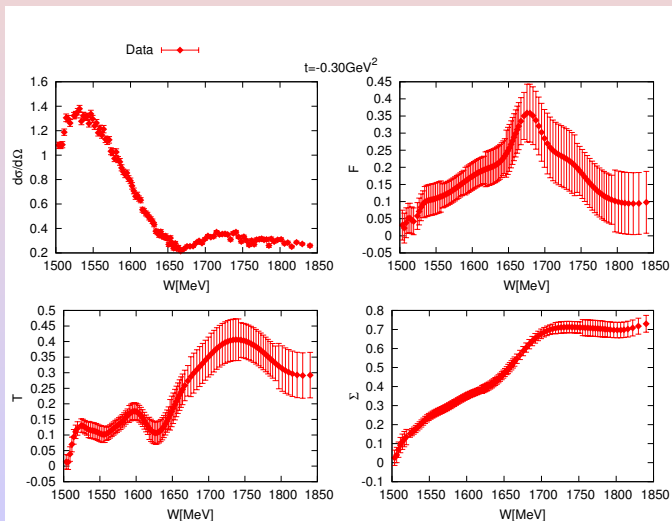
- Observables $\frac{d\sigma}{d\Omega}$, T , F and Σ are available at different t-values (different $\cos\theta$).
- Fixed-t amplitude analysis is performed at t-values in the range $-0.05 \text{ GeV}^2 < t < -1.00 \text{ GeV}^2$.
- Using spline fit, experimental data ($\frac{d\sigma}{d\Omega}$, T , F and Σ) are shifted to the predetermined t-values from above interval.



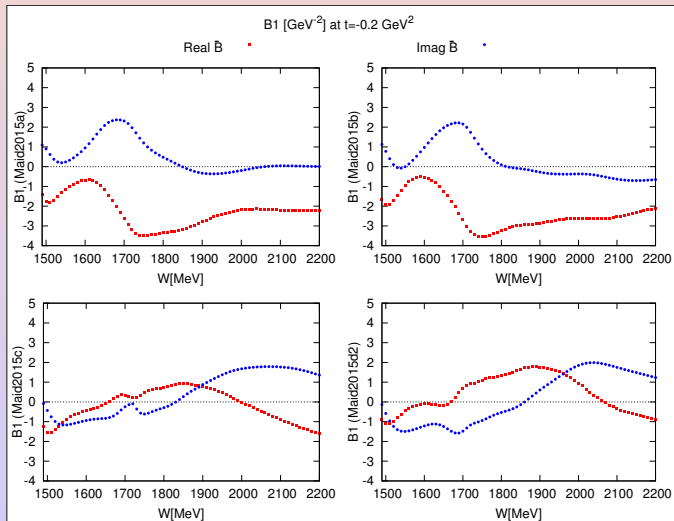
Interpolated values of measurable quantities at $t = -0.15 \text{ GeV}^2$



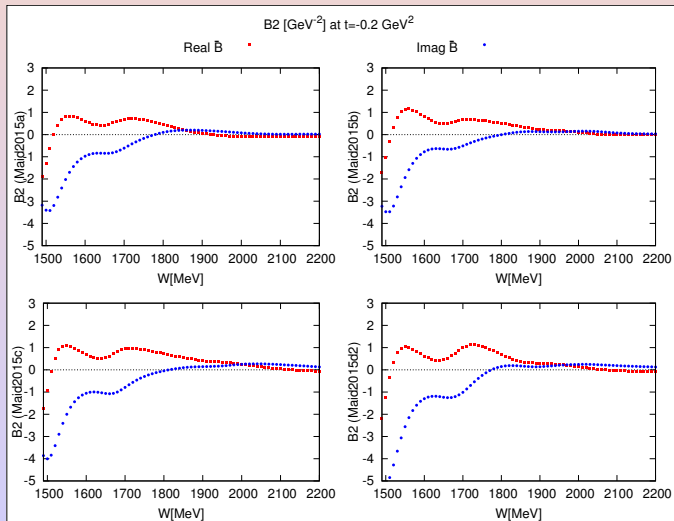
Interpolated values of measurable quantities at $t = -0.30 \text{ GeV}^2$



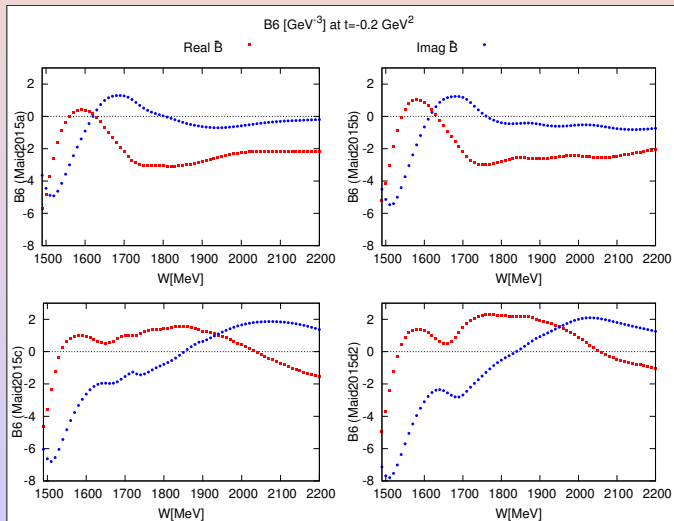
MAID15 solutions-comparison of invariant amplitudes



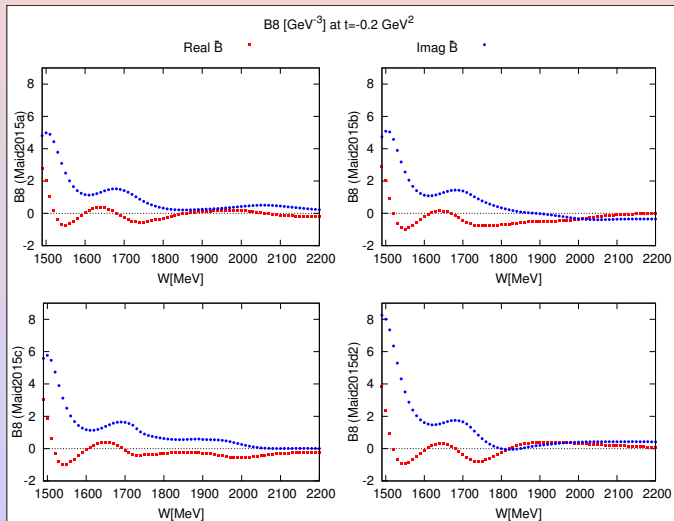
MAID15 solutions-comparison of invariant amplitudes



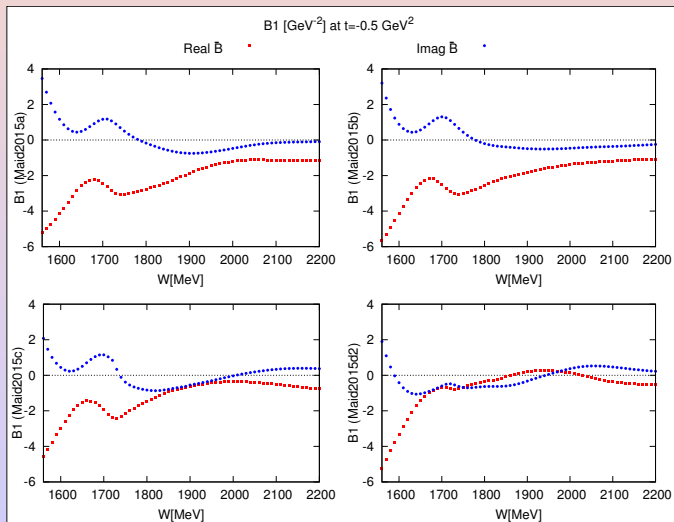
MAID15 solutions-comparison of invariant amplitudes



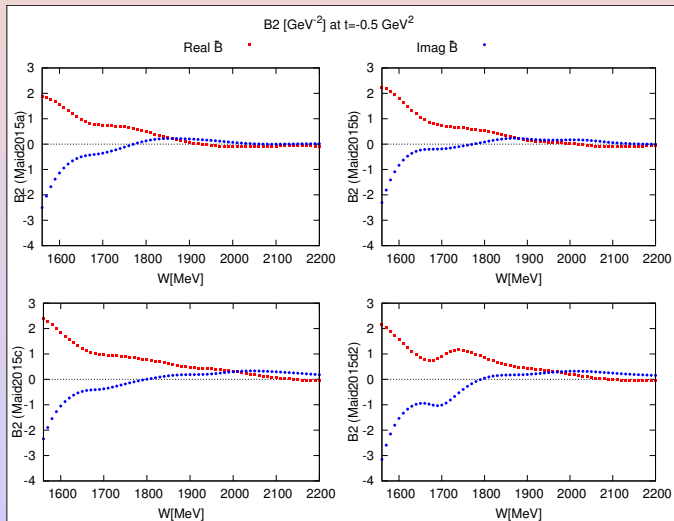
MAID15 solutions-comparison of invariant amplitudes



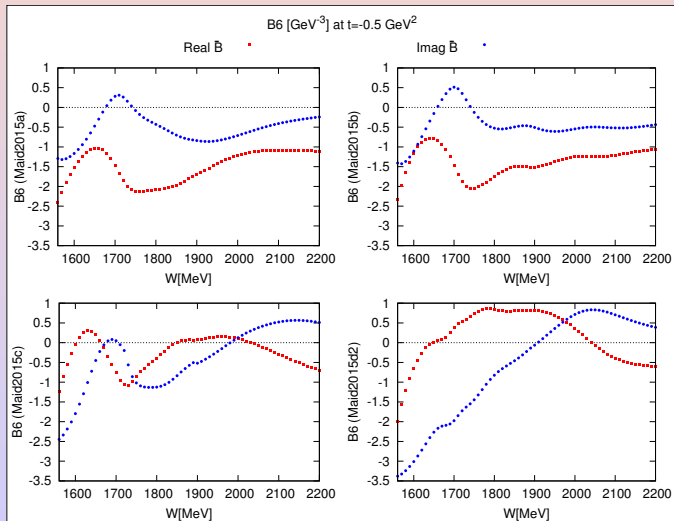
MAID15 solutions-comparison of invariant amplitudes



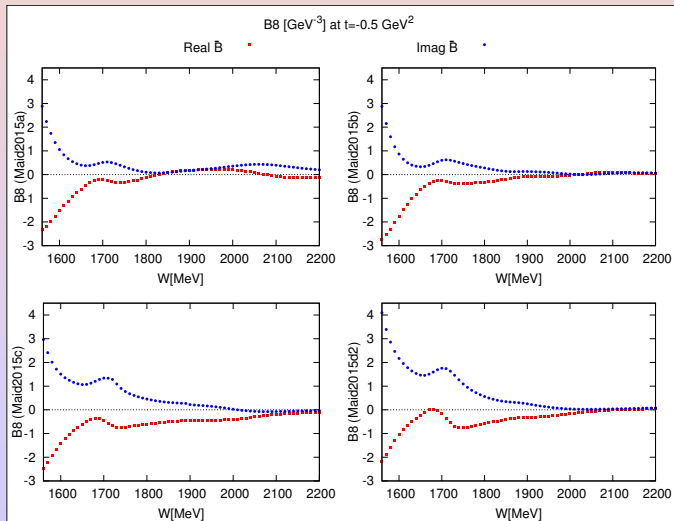
MAID15 solutions-comparison of invariant amplitudes



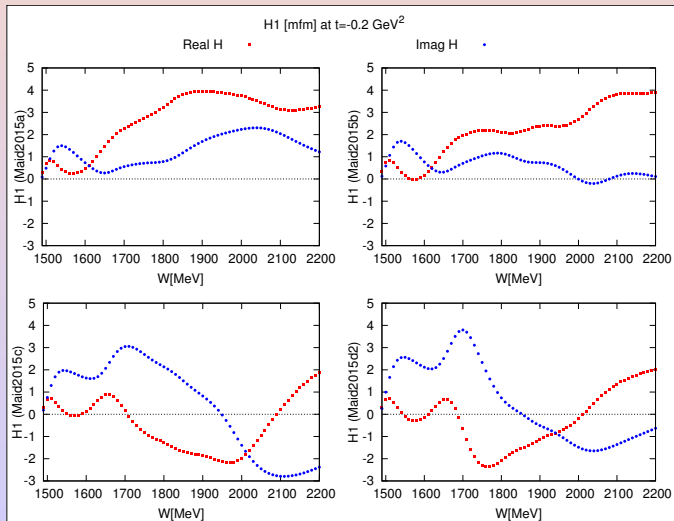
MAID15 solutions-comparison of invariant amplitudes



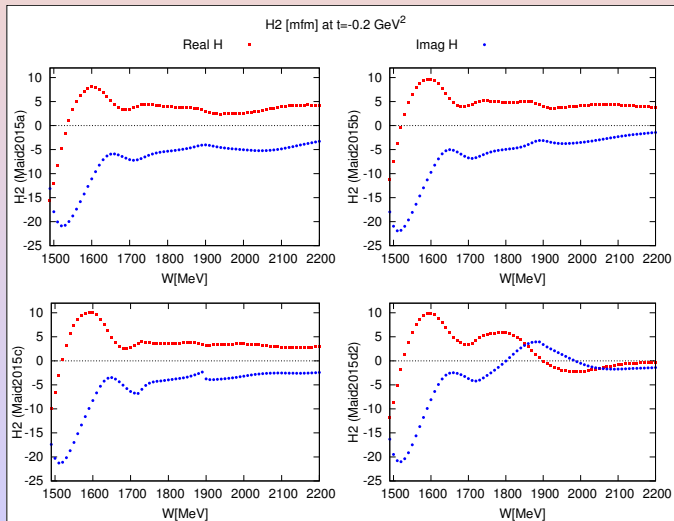
MAID15 solutions-comparison of invariant amplitudes



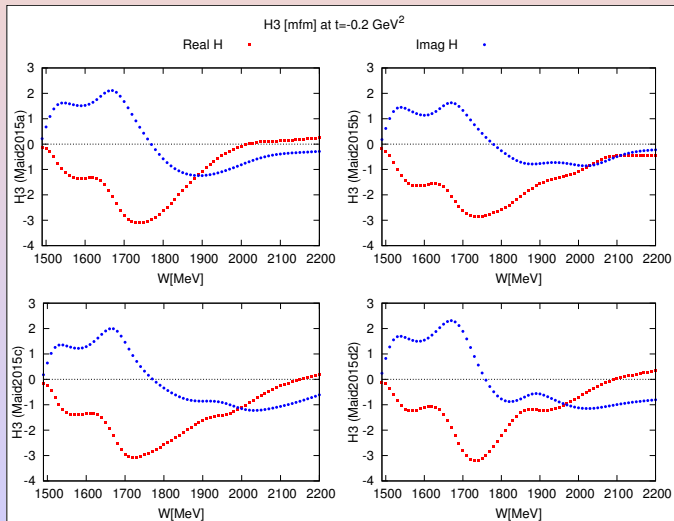
MAID15 solutions-comparison of helicity amplitudes



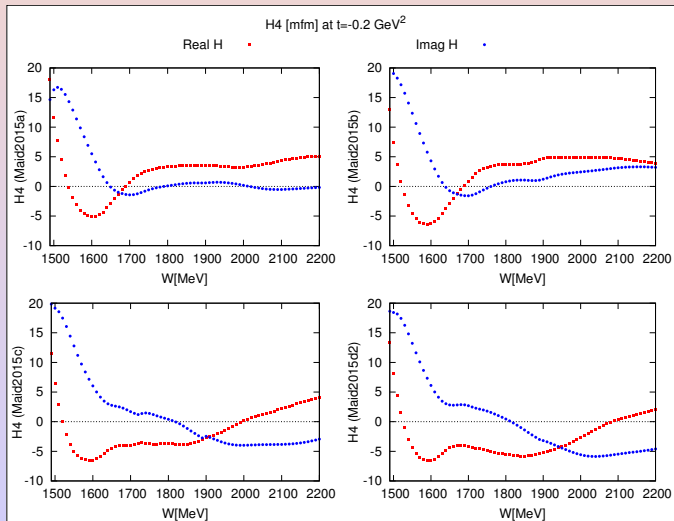
MAID15 solutions-comparison of helicity amplitudes



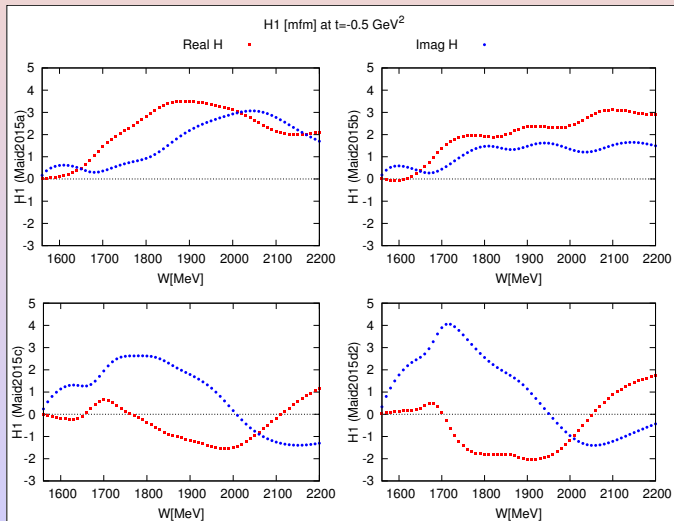
MAID15 solutions-comparison of helicity amplitudes



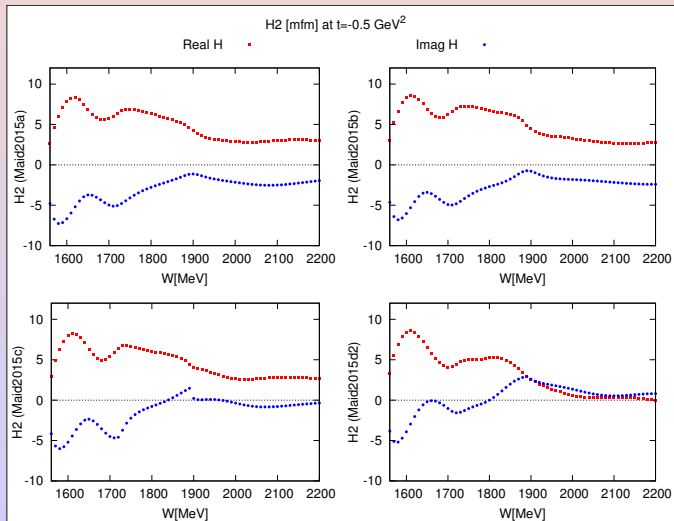
MAID15 solutions-comparison of helicity amplitudes



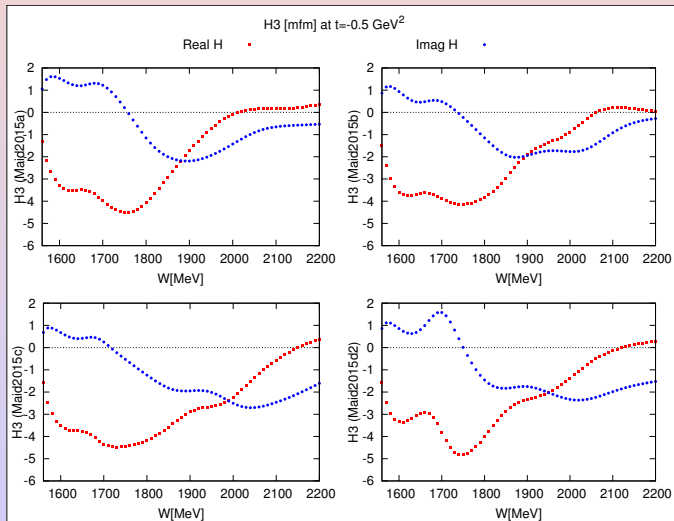
MAID15 solutions-comparison of helicity amplitudes



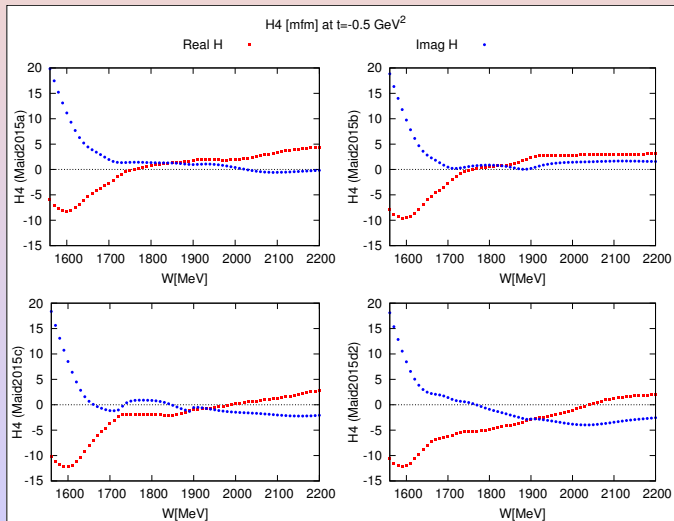
MAID15 solutions-comparison of helicity amplitudes



MAID15 solutions-comparison of helicity amplitudes



MAID15 solutions-comparison of helicity amplitudes



A quick check of consistency of MAID15 solutions with fixed-t analyticity.

$$\text{Re}\bar{B}_i(\nu^2, t) = \frac{1}{\pi} \int_{\nu_{th1}^2}^{\nu_{th2}^2} \frac{\text{Im}B_i(\nu'^2, t)}{\nu'^2 - \nu^2} d\nu'^2 + \frac{1}{\pi} \int_{\nu_{th2}^2}^{\infty} \frac{\text{Im}B_i(\nu'^2, t)}{\nu'^2 - \nu^2} d\nu'^2$$

$$\text{Re}\bar{B}_i(\nu^2, t) = \frac{1}{\pi} \int_{\nu_{th2}^2}^{\nu_{max}^2} \frac{\text{Im}B_i(\nu'^2, t)}{\nu'^2 - \nu^2} d\nu'^2 + \text{Dis} = \text{PVI} + \text{Dis}$$

$$\nu_{th1} = \frac{2(m + m_\pi)^2 - \Sigma - t}{4m}, \nu_{th2} = \frac{2(m + m_\eta)^2 - \Sigma - t}{4m}, \Sigma = 2m^2 + m_\eta^2$$

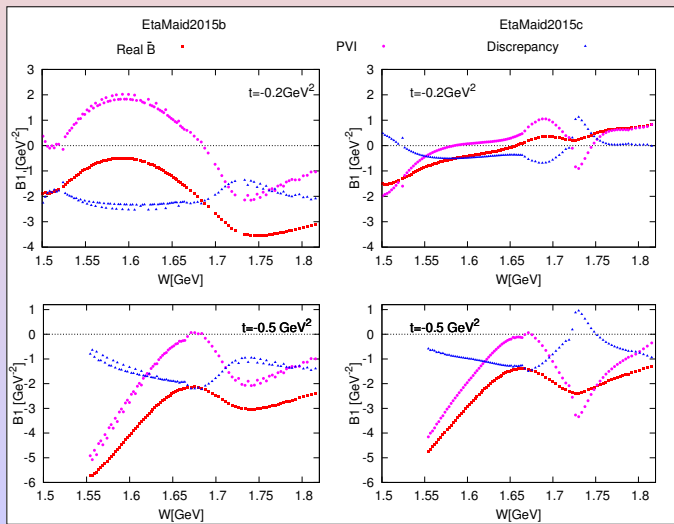
$$\text{Dis} = \text{Re}\bar{B}_i(\nu^2, t) - \boxed{\frac{1}{\pi} \int_{\nu_{th1}^2}^{\nu_{th2}^2} \frac{\text{Im}B_i(\nu'^2, t)}{\nu'^2 - \nu^2} d\nu'^2} - \frac{1}{\pi} \int_{\nu_{max}^2}^{\infty} \frac{\text{Im}B_i(\nu'^2, t)}{\nu'^2 - \nu^2} d\nu'^2$$

PVI - principal value integral. Dis should be smooth function without



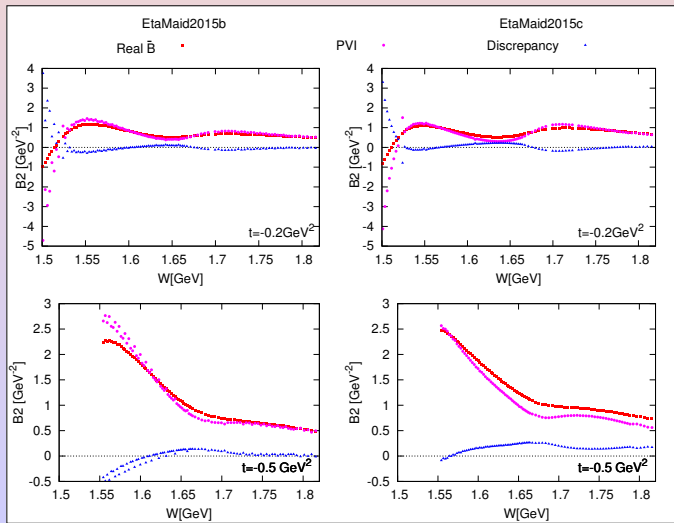
Check of fixed-t analyticity - FTDR

B_1



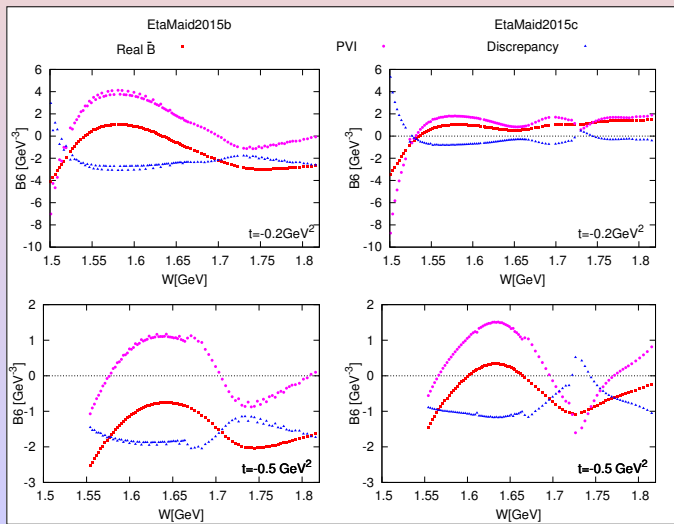
Check of fixed-t analyticity - FTDR

B_2



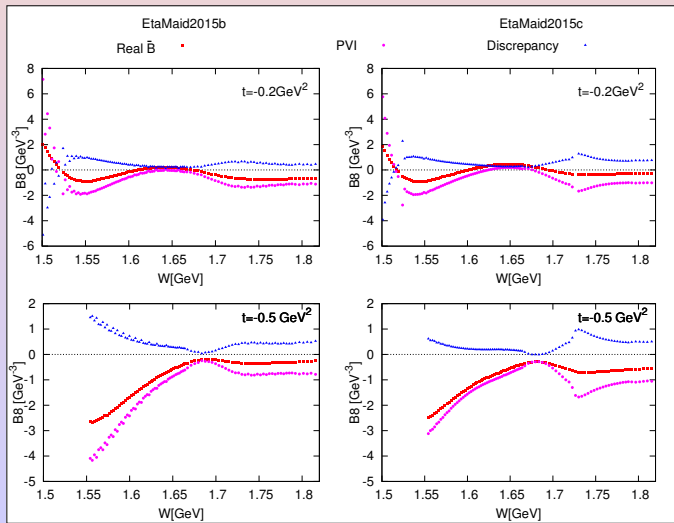
Check of fixed-t analyticity - FTDR

B_6



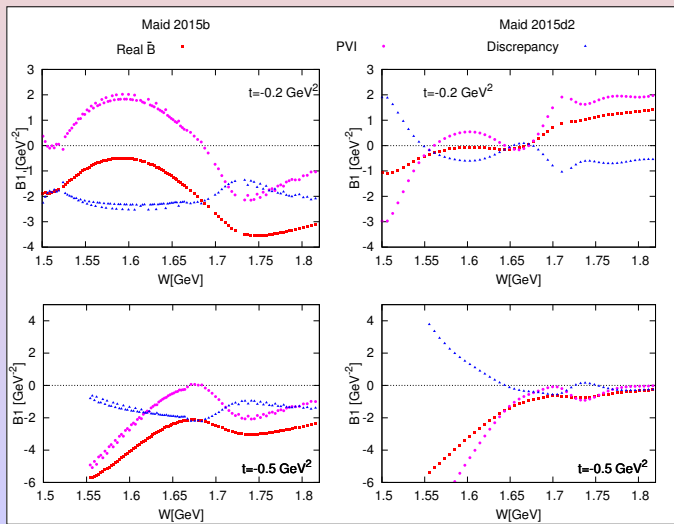
Check of fixed-t analyticity -FTDR

B_8



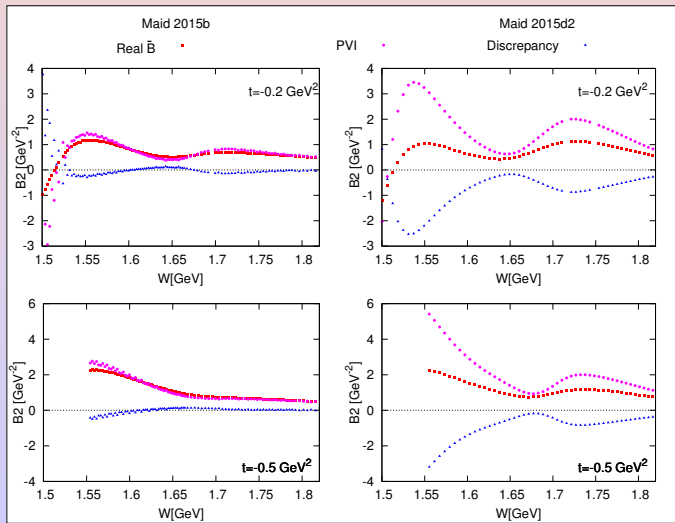
Check of fixed-t analyticity - FTDR

B_1



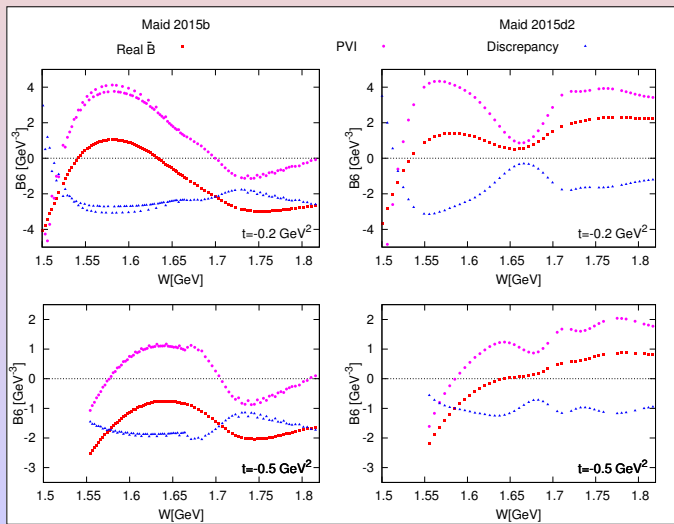
Check of fixed-t analyticity - FTDR

B_2



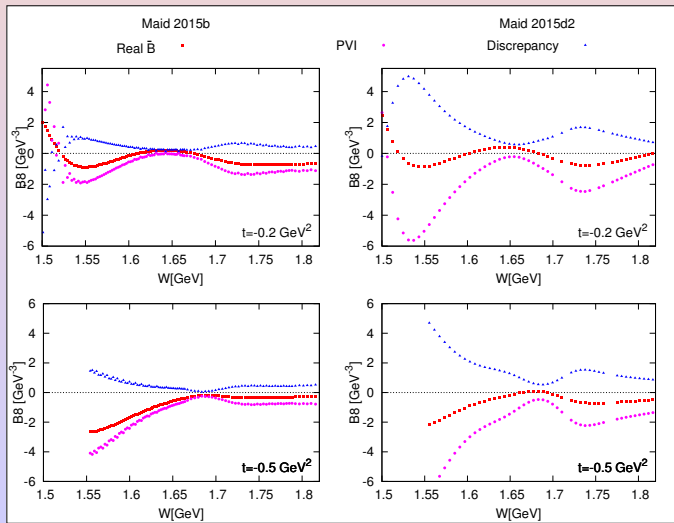
Check of fixed-t analyticity - FTDR

B_6



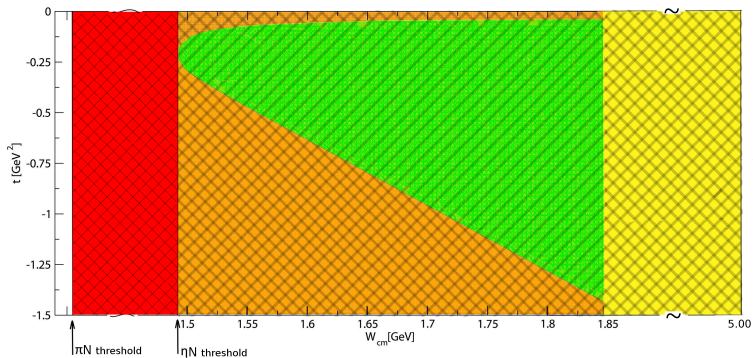
Check of fixed-t analyticity - FTDR

B_8



Check of fixed-t analyticity - FTDR

Important contributions are missing.



In present calculations 4 observables were fitted: $d\sigma/d\Omega$, F, T and Σ .

$$\chi^2 = \chi_{data}^2 + \chi_{PW}^2 + \Phi$$

$$\chi_{PW}^2 = q \sum_{k=1}^4 \sum_{n=1}^{N_{th}} \left[\left(\frac{\text{Re}H_k(\omega, x_n)^{fit} - \text{Re}H_k(\omega, x_n)^{start}}{\varepsilon_{k,n}^{Re}} \right)^2 + \left(\frac{\text{Im}H_k(\omega, x_n)^{fit} - \text{Im}H_k(\omega, x_n)^{start}}{\varepsilon_{k,n}^{Im}} \right)^2 \right]$$

H_k -helicity amplitudes from SE ($-0.09 \text{ GeV}^2 > t > -1.00 \text{ GeV}^2$)

q - adjustable weight factor. ($q = 1.0$).

$\varepsilon_{k,n}^{Re}$ and $\varepsilon_{k,n}^{Im}$ are errors. In this case $\varepsilon = \varepsilon_{k,n}^{Im} = 1.0$.



Pietarinen expansion of invariant amplitudes

We use Pietarinen's expansion with two thresholds (πN and ηN) and two conformal variables

$$z_1 = \frac{\alpha - \sqrt{\nu_{th1}^2 - \nu^2 - i \cdot eps}}{\alpha + \sqrt{\nu_{th1}^2 - \nu^2 - i \cdot eps}} \quad z_2 = \frac{\beta - \sqrt{\nu_{th2}^2 - \nu^2 - i \cdot eps}}{\beta + \sqrt{\nu_{th2}^2 - \nu^2 - i \cdot eps}}$$

$$\alpha = \beta = 0.9, Th(\pi N) = 1.07325 \text{ GeV}, Th(\eta N) = 1.486 \text{ GeV}. \nu = \frac{s-u}{4m}$$

$$B_1 = B_{1N} + P_R(z_1) \cdot (1 + z_1) \cdot \sum_i b_{1i}^{(1)} z_1^i + (1 + z_2) \cdot \sum_i b_{1i}^{(2)} z_2^i$$

$$B_2 = B_{2N} + P_R(z_1) \cdot (1 + z_1) \cdot \sum_i b_{2i}^{(1)} z_1^i + (1 + z_2) \cdot \sum_i b_{2i}^{(2)} z_2^i$$

$$B_6 = B_{6N} + P_R(z_1) \cdot (1 + z_1) \cdot \sum_i b_{6i}^{(1)} z_1^i + (1 + z_2) \cdot \sum_i b_{6i}^{(2)} z_2^i$$

$$\frac{B_8}{\nu} = \frac{B_{8N}}{\nu} + P_R(z_1) \cdot (1 + z_1) \cdot \sum_i b_{8i}^{(1)} z_1^i + (1 + z_2) \cdot \sum_i b_{8i}^{(2)} z_2^i$$



A factor

$$P_R(z_1) = \frac{(1 + z_R)(1 + z_R^*)}{(z_1 - z_R)(z_1 - z_R^*)},$$

was introduced to take into account contribution from the Roper resonance.

$$z_R = \frac{\alpha - \sqrt{\nu_{th1}^2 - \nu_R^2}}{\alpha + \sqrt{\nu_{th1}^2 - \nu_R^2}}.$$

z_R is a value of conformal variable z at P_{11} pole
 $W_R = (1.365 - 0.095i) \text{ GeV}$.



Dependence of amplitude solution on initial PW solution and PW constraint

Fixed-t invariant amplitudes $t = -0.20 \text{ GeV}^2$ (EtaMAID15b)

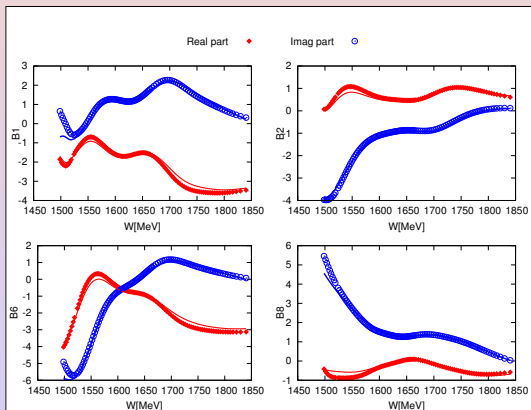


Figure : Corresponding fixed-t invariant amplitudes are obtained using initial solution etaMAID2015b (red diamonds and blue circles). Red and blue solid lines are fits of invariant amplitudes B_i .



Fixed-t invariant amplitudes $t = -0.20 \text{ GeV}^2$ (EtaMAID15d2)

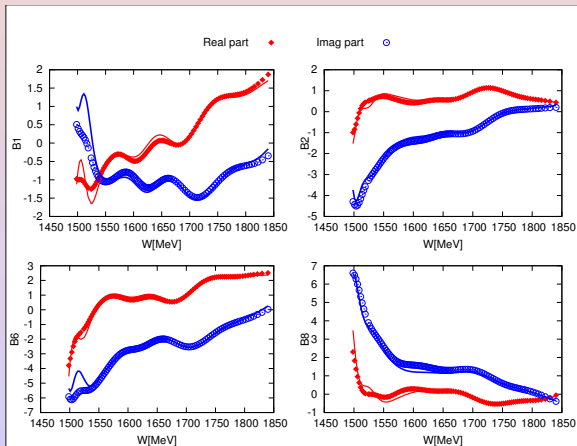


Figure : Corresponding fixed-t invariant amplitudes are obtained using initial solution etaMAID2015d2 (red diamonds and blue circles). Red and blue solid lines are fits of invariant amplitudes B_i .



Fixed- t invariant amplitudes $t = -0.50\text{GeV}^2$ (EtaMAID15b)

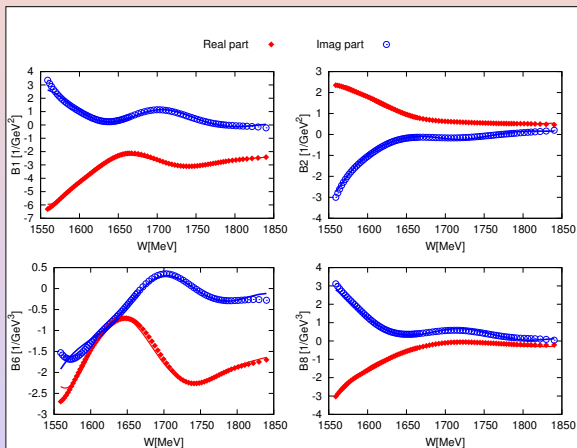


Figure : Corresponding fixed- t invariant amplitudes are obtained using initial solution etaMAID2015b (red diamonds and blue circles). Red and blue solid lines are fits of invariant amplitudes B_i .



Fixed-t invariant amplitudes

$t = -0.50 \text{ GeV}^2$ (EtaMAID15d2)

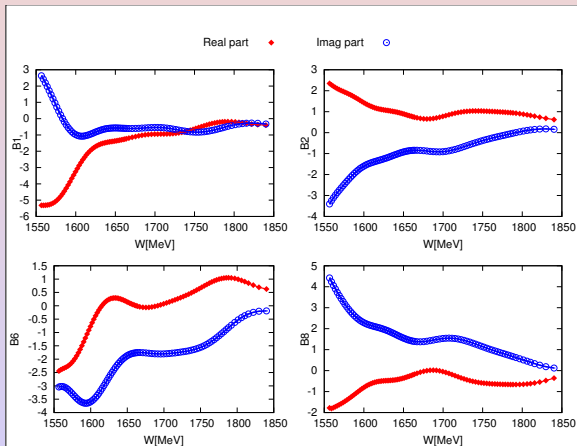


Figure : Corresponding fixed-t invariant amplitudes are obtained using initial solution etaMAID2015d2 (red diamonds and blue circles). Red and blue solid lines are fits of invariant amplitudes B_i .



Fixed- t invariant amplitudes $t = -1.00\text{GeV}^2$ (EtaMAID15b)

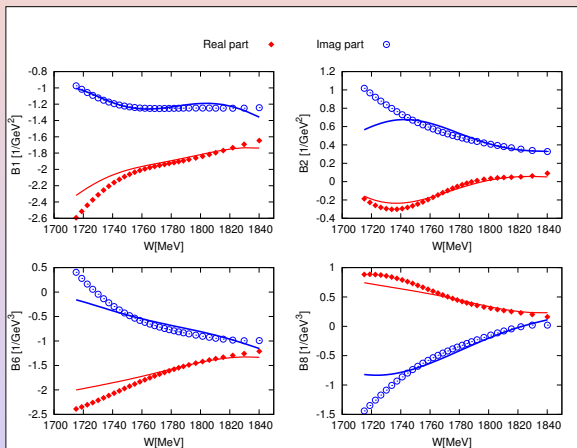


Figure : Corresponding fixed- t invariant amplitudes are obtained using initial solution etaMAID2015b (red diamonds and blue circles). Red and blue solid lines are fits of invariant amplitudes B_i .



Fixed-t invariant amplitudes $t = -1.00 \text{ GeV}^2$ (EtaMAID15d2)

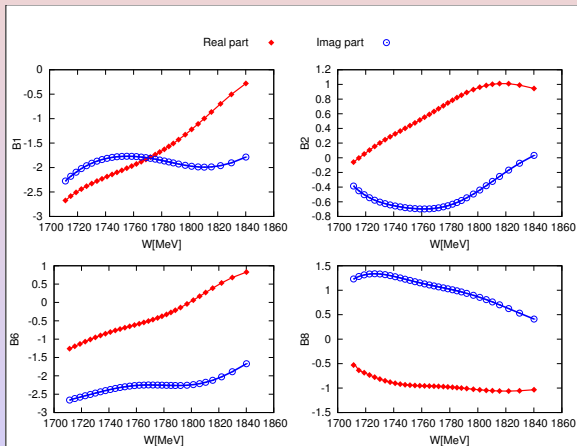
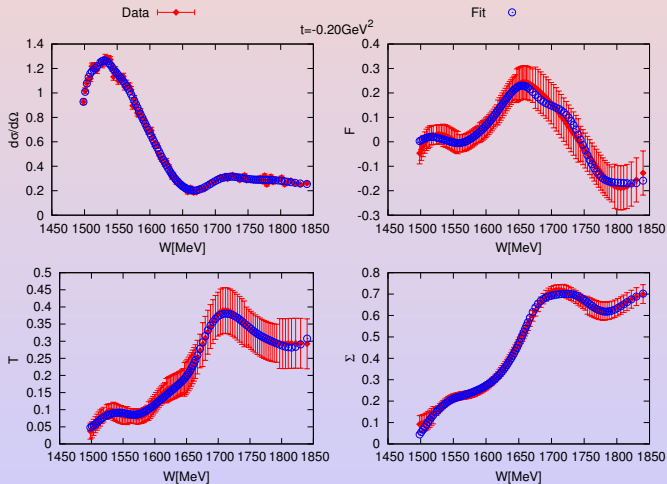


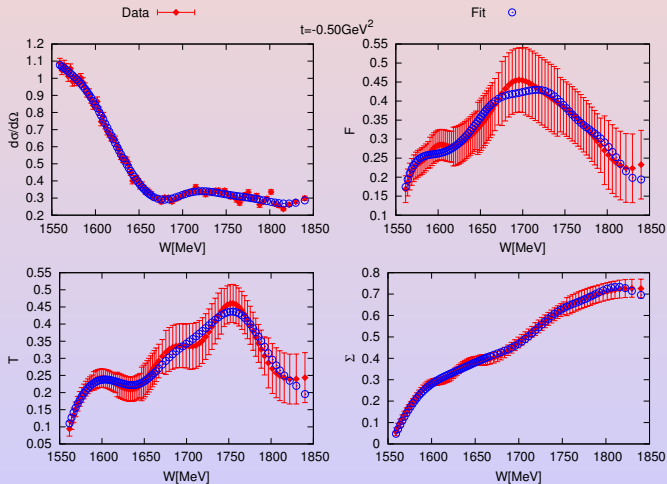
Figure : Corresponding fixed-t invariant amplitudes are obtained using initial solution etaMAID2015d2 (red diamonds and blue circles). Red and blue solid lines are fits of invariant amplitudes B_i .



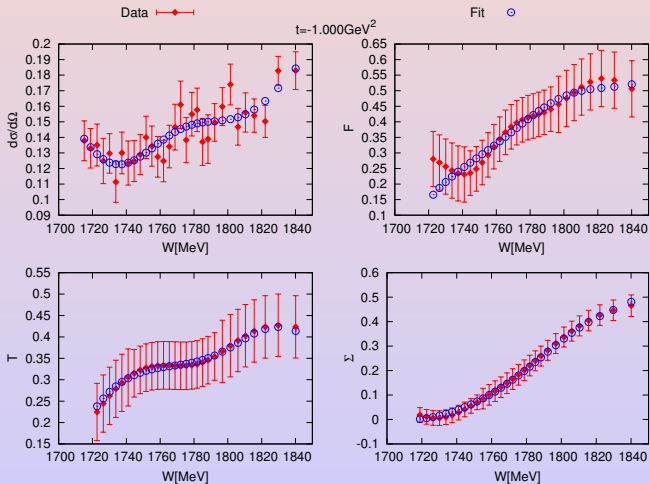
Fit of experimental data $t = -0.20\text{GeV}^2$ (EtaMAID15b)



Fit of experimental data $t = -0.50\text{GeV}^2$ (EtaMAID15b)



Fit of experimental data $t = -1.0 \text{ GeV}^2$ (EtaMAID15b)



We present SE fits to the real data. In present calculations 4 observables were fitted: $d\sigma/d\Omega$, $\Sigma d\sigma/d\Omega$, $Td\sigma/d\Omega$ and $Fd\sigma/d\Omega$.

Multipoles up to H-waves ($l = 5$) were fitted.

$$\chi^2 = \chi_{data}^2 + \chi_{PW}^2 + \Phi_{trunc}$$

$$\chi_{PW}^2 = q \sum_{k=1}^4 \sum_{n=1}^{N_{th}} \left[\left(\frac{\text{Re}H_k(\omega, x_n)^{fit} - \text{Re}H_k(\omega, x_n)^{start}}{\varepsilon_{k,n}^{Re}} \right)^2 + \left(\frac{\text{Im}H_k(\omega, x_n)^{fit} - \text{Im}H_k(\omega, x_n)^{start}}{\varepsilon_{k,n}^{Im}} \right)^2 \right]$$

H_k -helicity amplitudes from FT ($-0.09 \text{ GeV}^2 > t > -1.00 \text{ GeV}^2$). As a constraint we used etaMAID2015a.

q - adjustable weight factor. ($q = 1.5$).

$\varepsilon_{k,n}^{Re}$ and $\varepsilon_{k,n}^{Im}$ are errors. In this case $\varepsilon_{k,n}^{Re} = \varepsilon_{k,n}^{Im} = 1$.



$$\Phi_{trunc} = \lambda \sum_{\ell=0}^{\ell_{max}} [|\operatorname{Re} T_{\ell\pm}|^2 R^{2\ell} + |\operatorname{Im} T_{\ell\pm}|^2 R^{2\ell}].$$

λ is adjustable weight factor ($\lambda = 0.3$ in present calculations.).

In a first attempt, we take $R = x_4 + \sqrt{x_4^2 - 1}$, where

$$x_4 = \cos \theta(t = 4m_\pi^2) = \frac{4m_\pi^2 - m_\eta^2 + 2k(s)\omega(s)}{2k(s)q(s)}.$$

$T_{\ell\pm}$ stands for electric and magnetic multipoles $E_{\ell\pm}$ and $M_{\ell\pm}$.

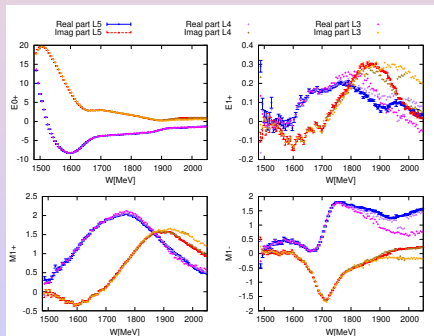


Smooth truncation-an example

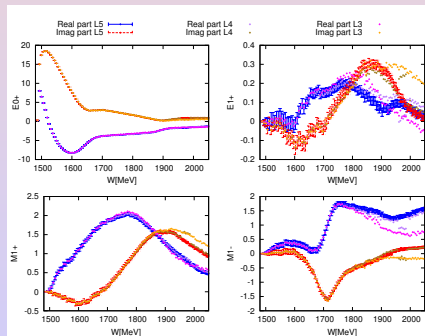
As example we show results obtained using etaMAID2015a pseudo data and etaMAID2015b as a constraint.

(a) $\chi^2 = \chi_{data}^2 + \chi_{FT}^2$

(b) $\chi^2 = \chi_{data}^2 + \chi_{FT}^2 + \Phi_{trunc}$



(a)



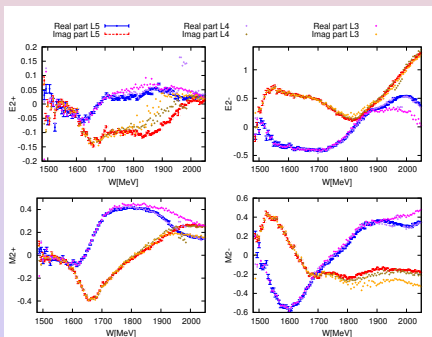
(b)



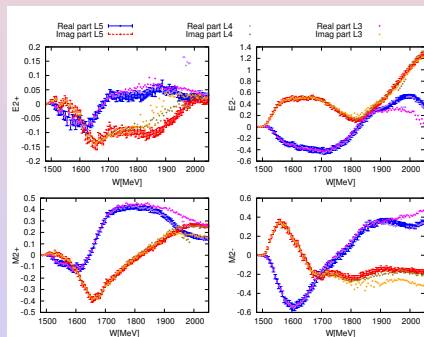
Smooth truncation-an example

(c) $\chi^2 = \chi^2_{data} + \chi^2_{FT}$

(d) $\chi^2 = \chi^2_{data} + \chi^2_{FT} + \Phi_{trunc}$



(c)



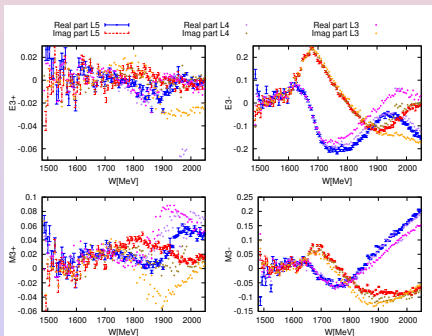
(d)



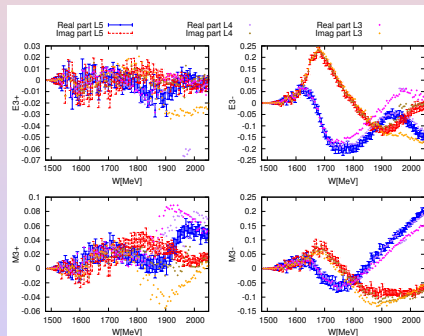
Smooth truncation-an example

$$(e) \chi^2 = \chi_{data}^2 + \chi_{FT}^2$$

$$(f) \chi^2 = \chi_{data}^2 + \chi_{FT}^2 + \Phi_{trunc}$$



(e)



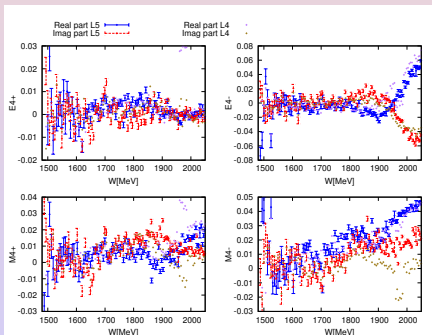
(f)



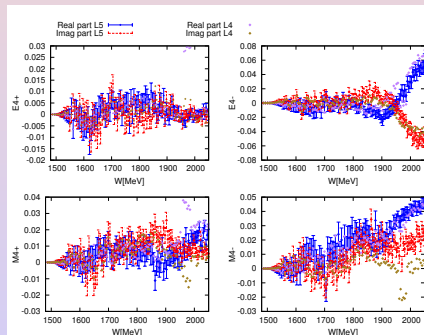
Smooth truncation-an example

$$(g) \chi^2 = \chi^2_{data} + \chi^2_{FT}$$

$$(h) \chi^2 = \chi^2_{data} + \chi^2_{FT} + \Phi_{trunc}$$



(g)



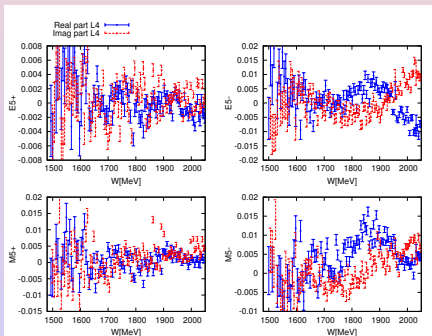
(h)



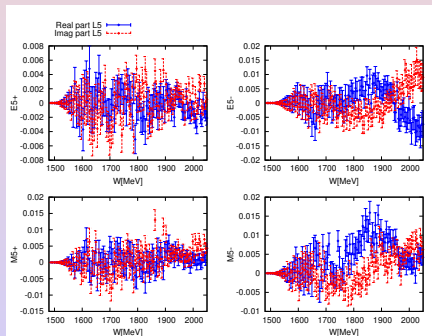
Smooth truncation-an example

$$(i) \chi^2 = \chi_{data}^2 + \chi_{FT}^2$$

$$(j) \chi^2 = \chi_{data}^2 + \chi_{FT}^2 + \Phi_{trunc}$$



(i)



(j)



SE PWA - Multipoles- Preliminary results

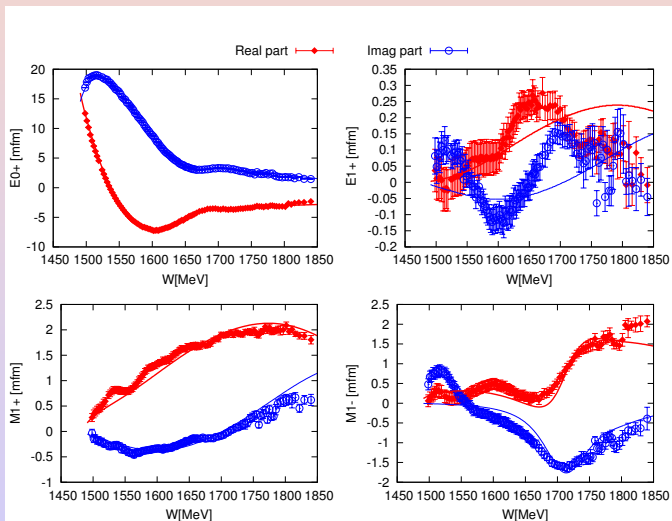


Figure : Red and blue solid lines-initial solution etaMAID2015a



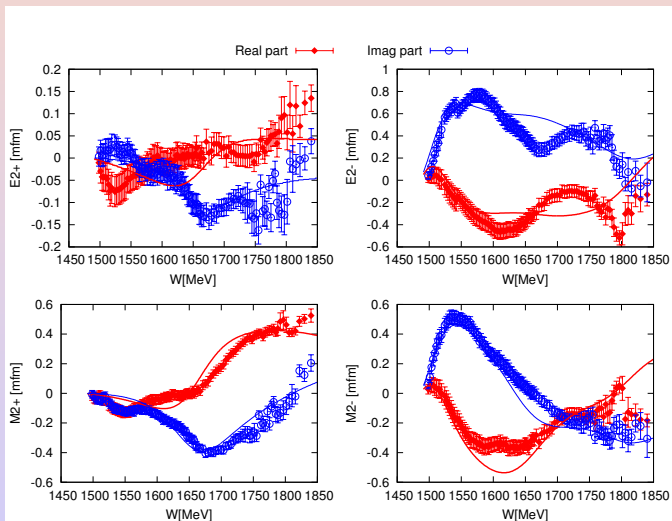


Figure : Red and blue solid lines-initial solution [etaMAID2015a](#)



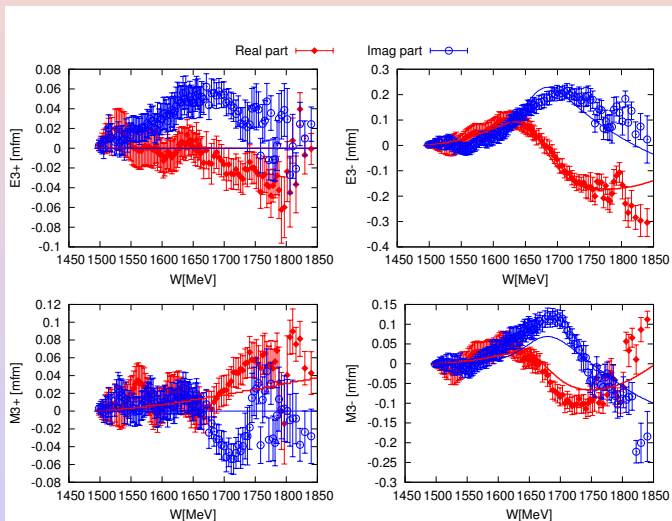


Figure : Red and blue solid lines-initial solution [etaMAID2015a](#)



SE PWA - Multipoles

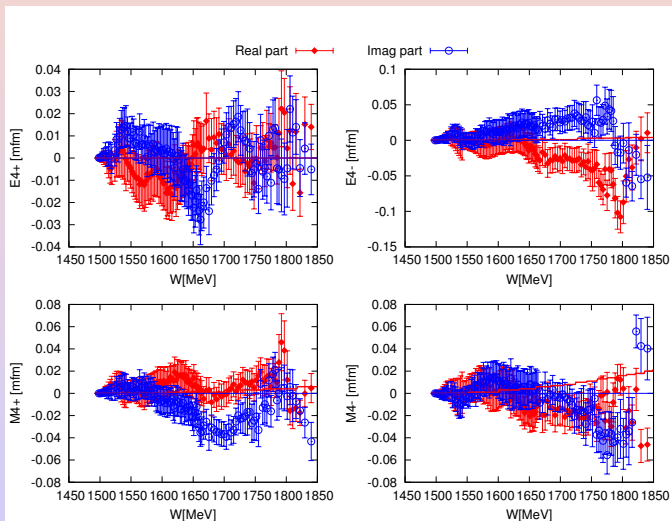


Figure : Red and blue solid lines-initial solution [etaMAID2015a](#)



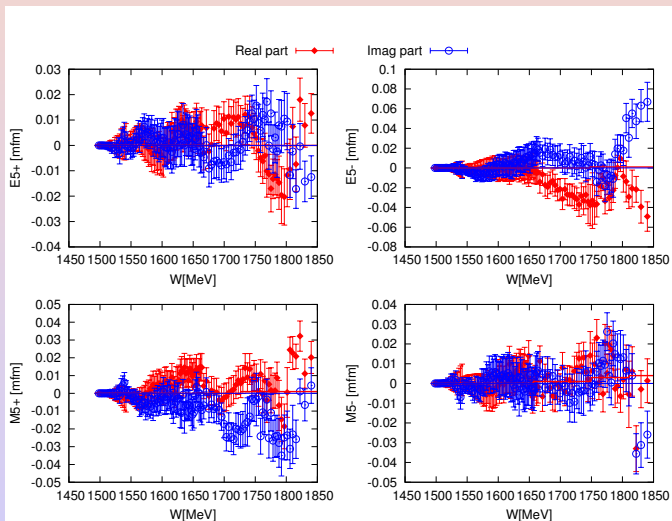
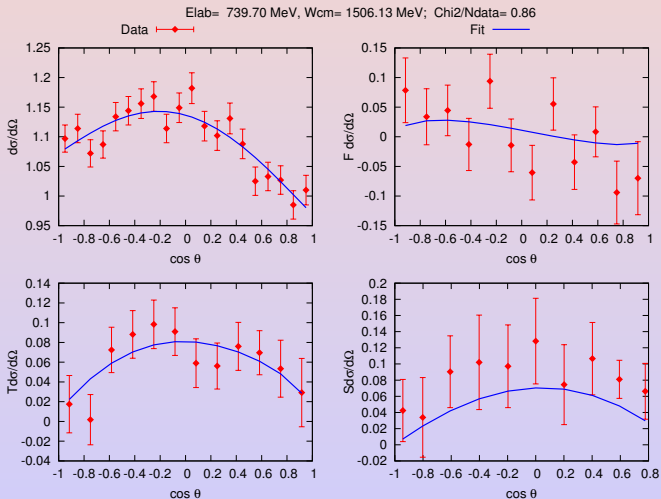
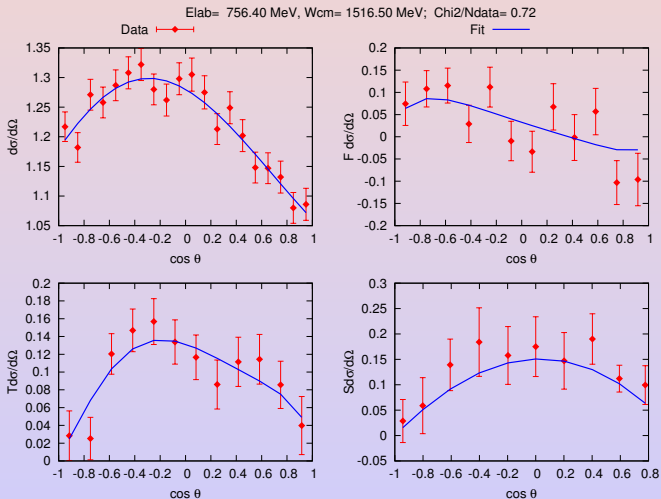
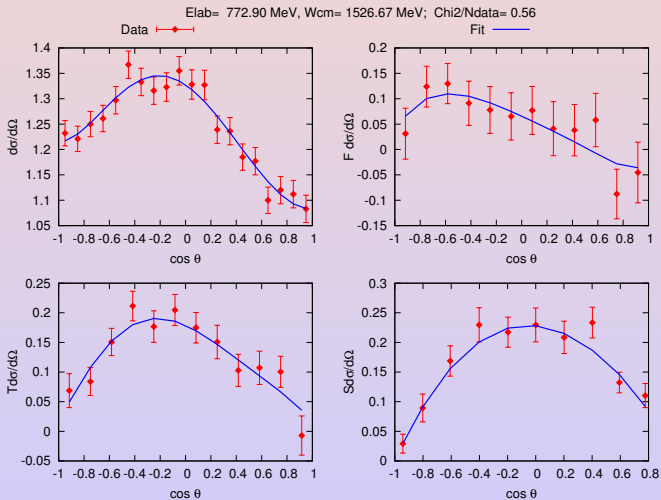


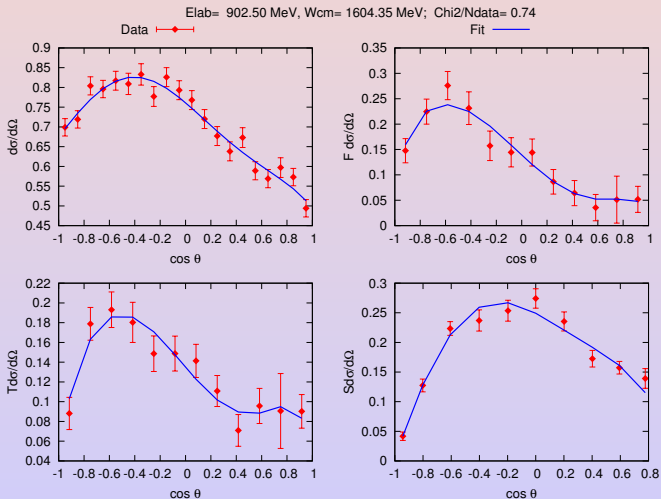
Figure : Red and blue solid lines-initial solution [etaMAID2015a](#)

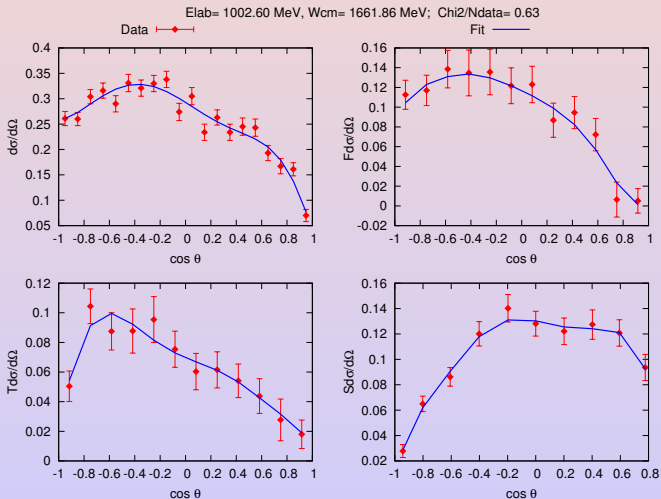


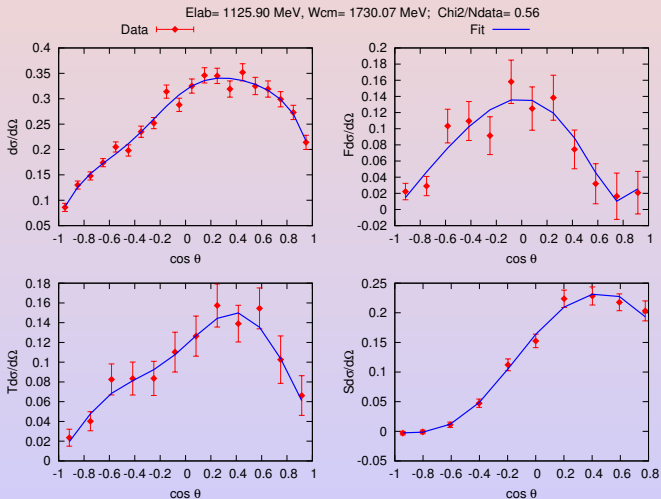


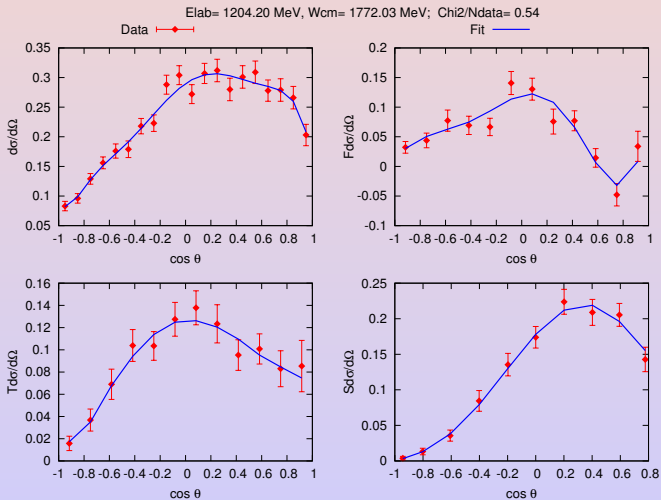


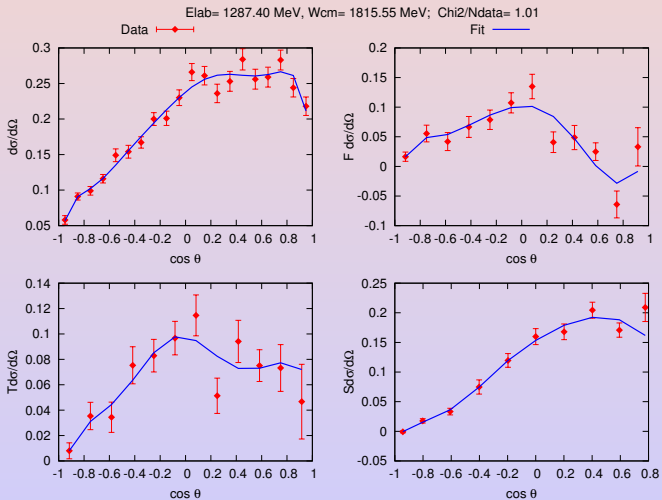


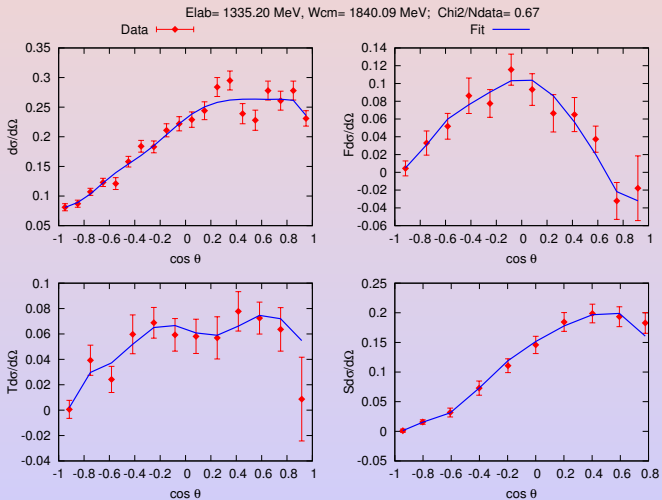




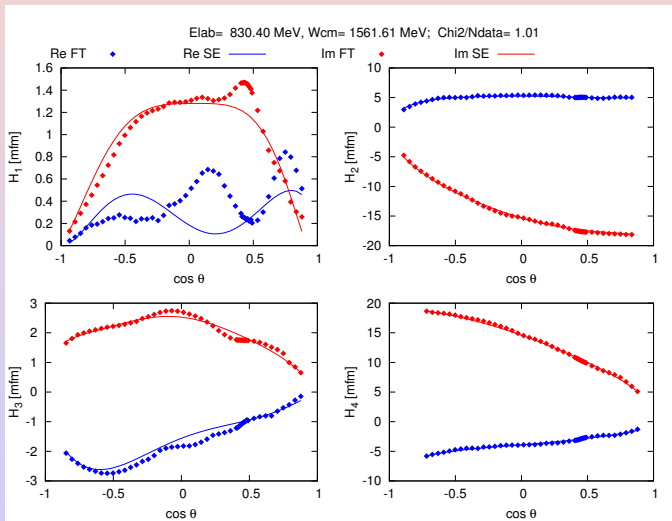




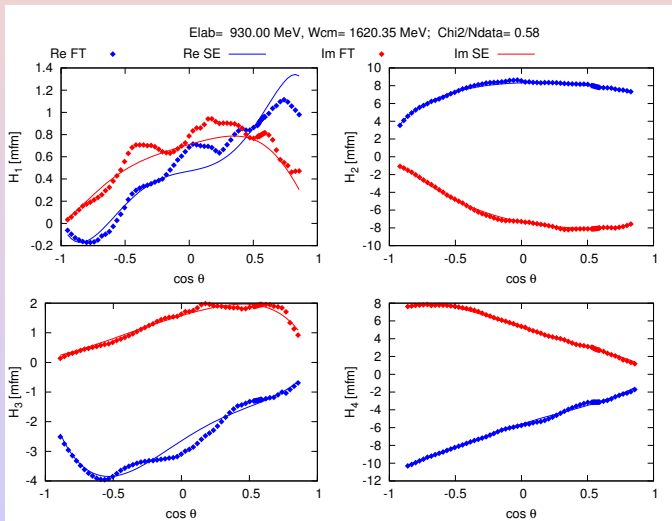




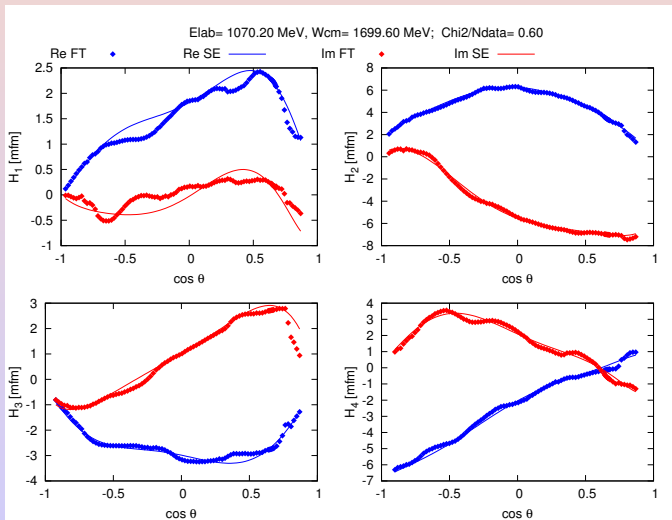
Helicity amplitudes



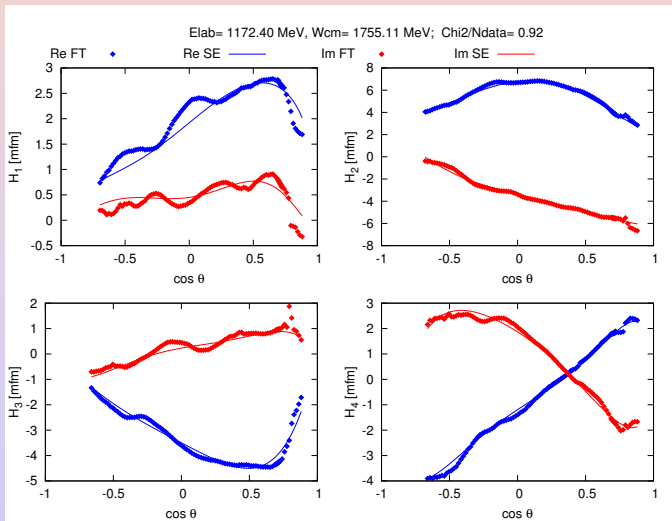
Helicity amplitudes



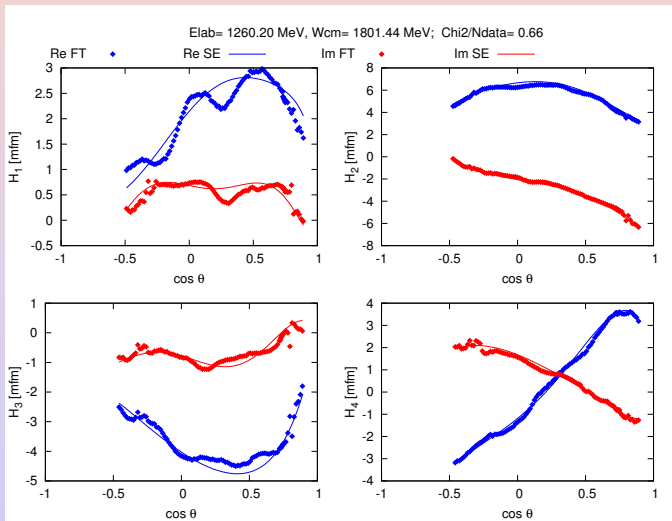
Helicity amplitudes



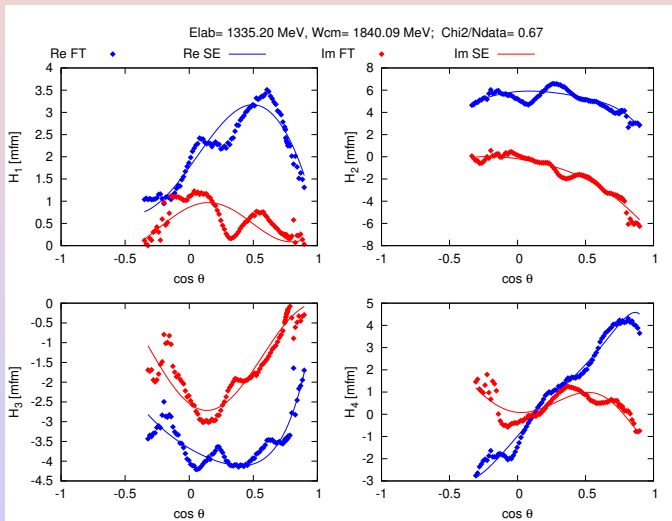
Helicity amplitudes



Helicity amplitudes



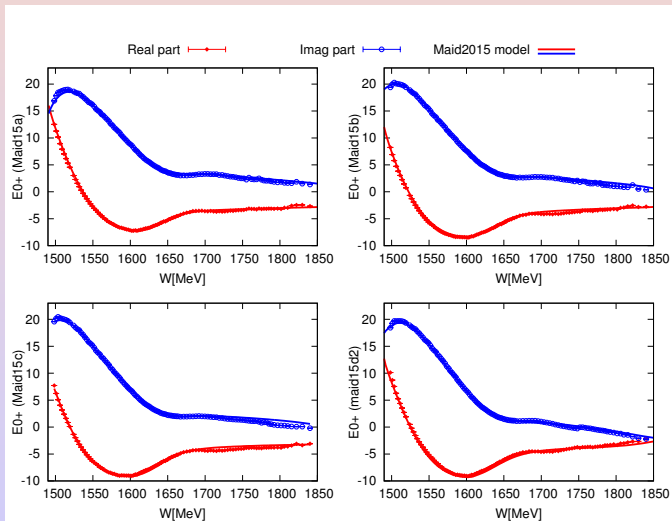
Helicity amplitudes



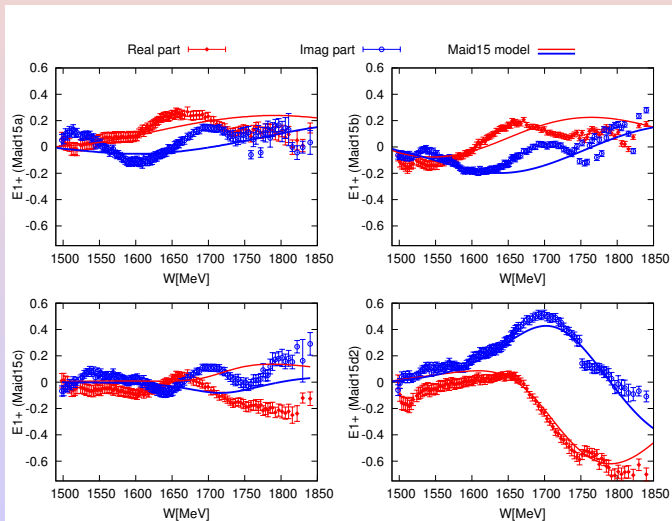
Problem: Dependence on constraining PW solution



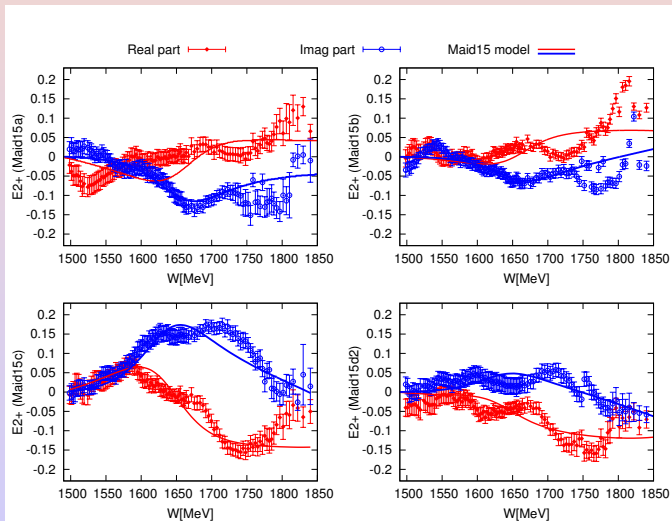
Dependance of SE PWA solution on constraint from FT AA



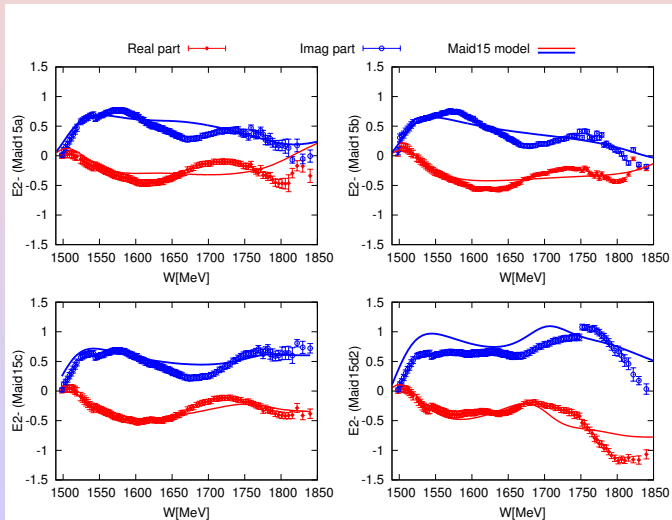
Dependance of SE PWA solution on constraint from FT AA



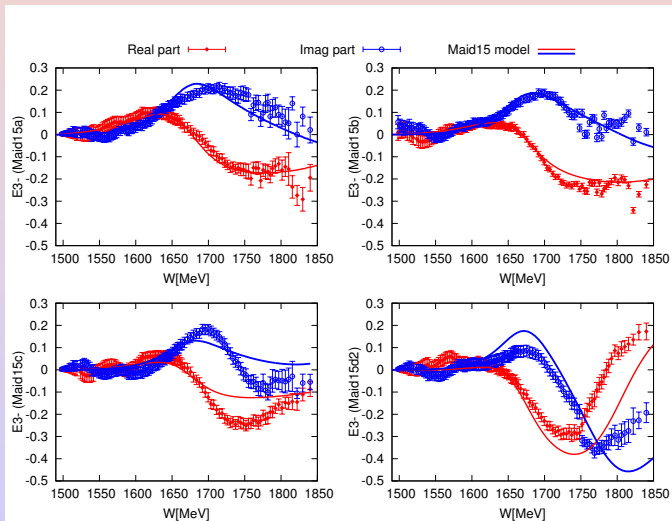
Dependance of SE PWA solution on constraint from FT AA



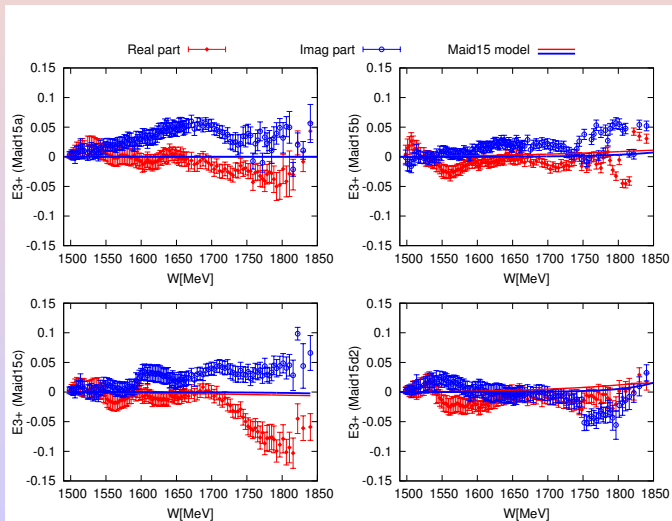
Dependance of SE PWA solution on constraint from FT AA



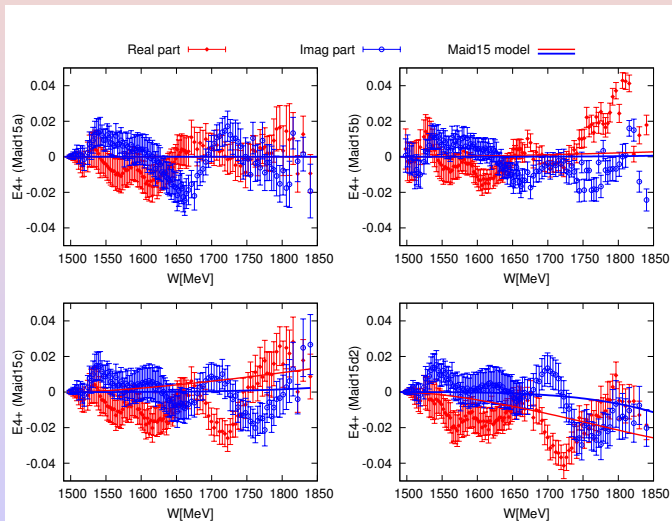
Dependance of SE PWA solution on constraint from FT AA



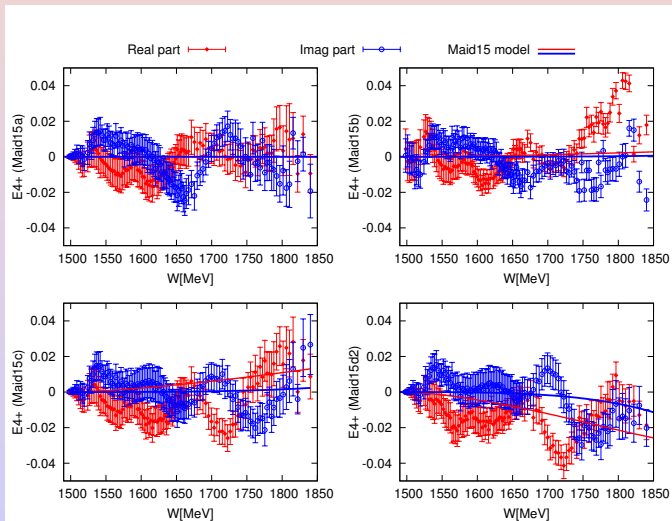
Dependance of SE PWA solution on constraint from FT AA



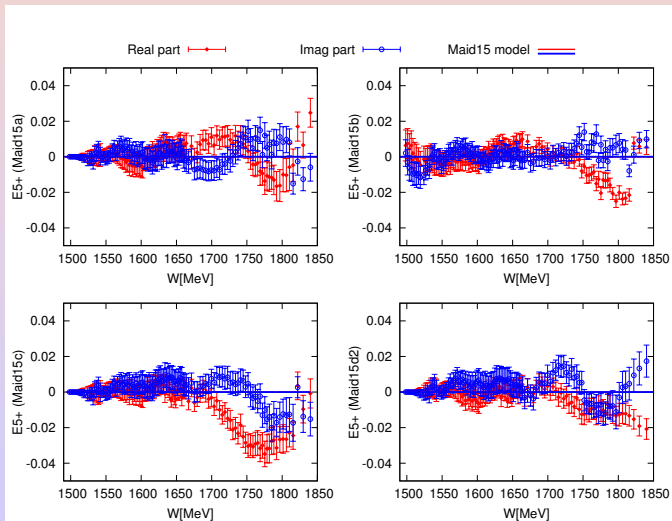
Dependance of SE PWA solution on constraint from FT AA



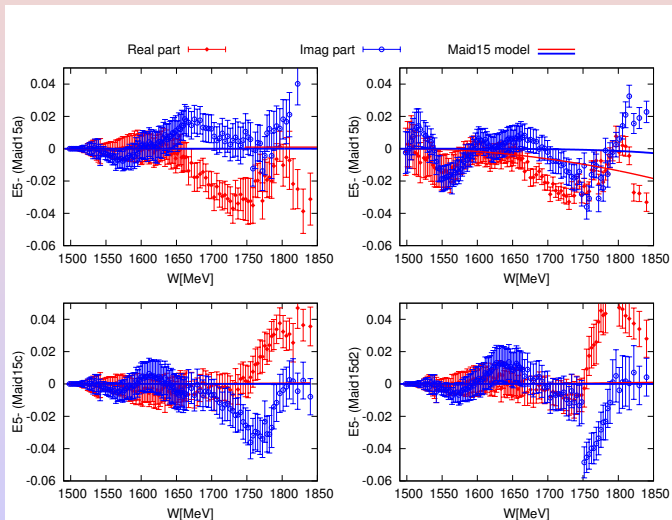
Dependance of SE PWA solution on constraint from FT AA



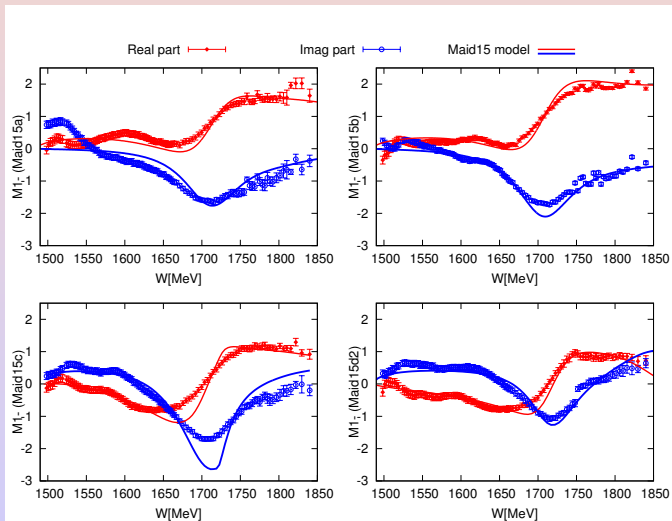
Dependance of SE PWA solution on constraint from FT AA



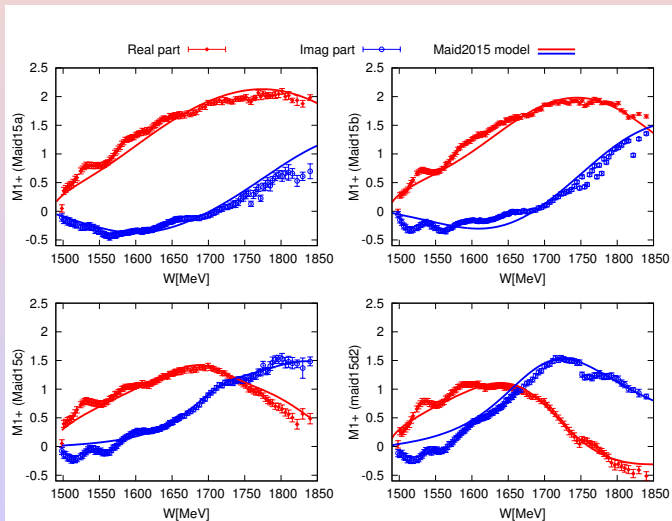
Dependance of SE PWA solution on constraint from FT AA



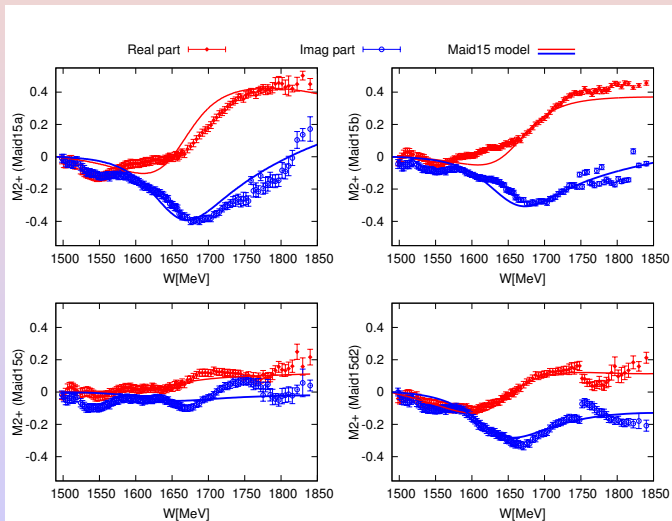
Dependance of SE PWA solution on constraint from FT AA



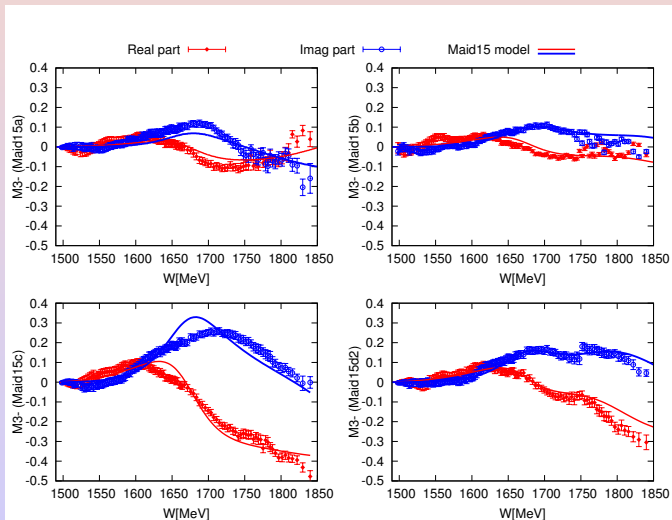
Dependance of SE PWA solution on constraint from FT AA



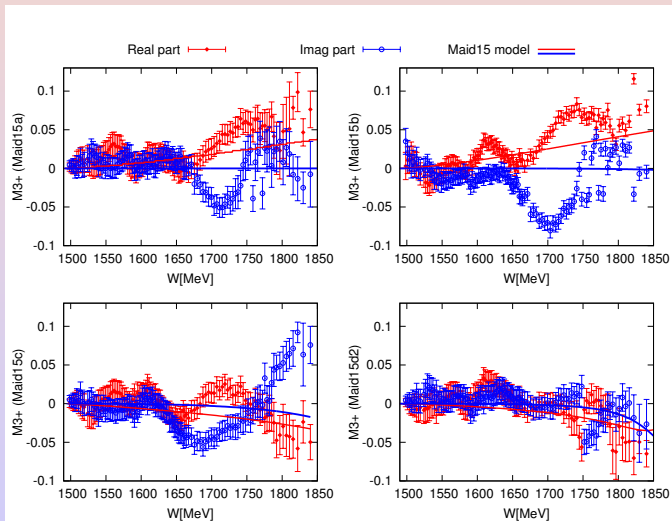
Dependance of SE PWA solution on constraint from FT AA



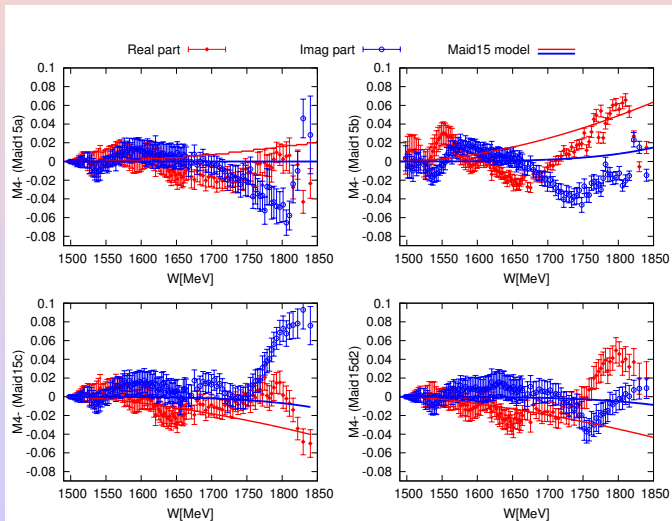
Dependance of SE PWA solution on constraint from FT AA



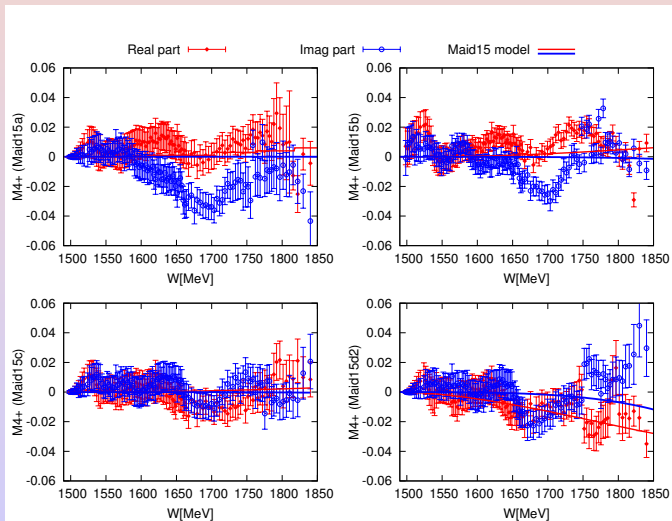
Dependance of SE PWA solution on constraint from FT AA



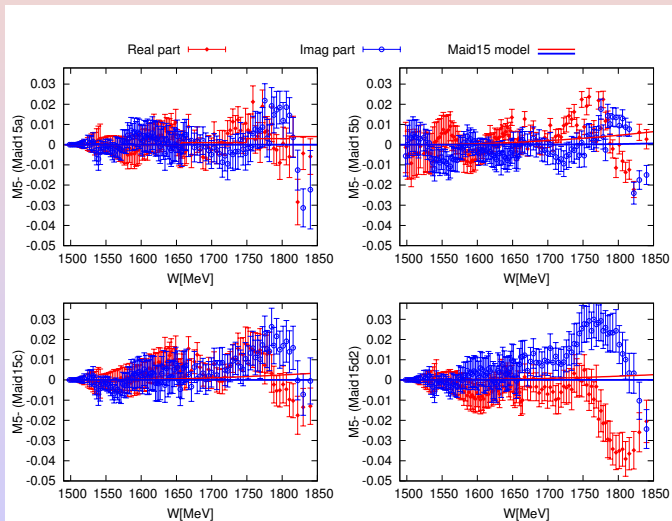
Dependance of SE PWA solution on constraint from FT AA



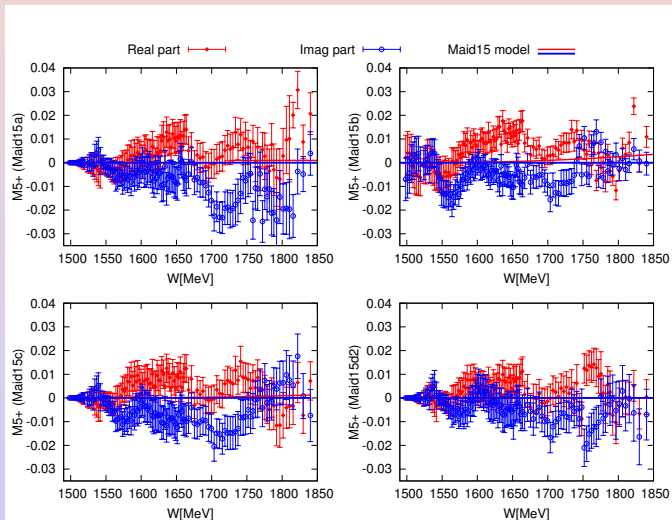
Dependance of SE PWA solution on constraint from FT AA



Dependance of SE PWA solution on constraint from FT AA



Dependance of SE PWA solution on constraint from FT AA



Search for unique solution



$$E_{0+}(W) = |E_{0+}(W)|e^{i\phi_0}$$

$$E_{\ell\pm}(W) = |E_{\ell\pm}(W)|e^{i\phi_\ell}$$

$$M_{\ell\pm}(W) = |M_{\ell\pm}(W)|e^{i\phi_\ell}$$

Reduced multipoles are

$$\tilde{E}_{\ell\pm}(W) = |E_{\ell\pm}(W)|e^{i(\phi_\ell - \phi_0)}, \quad \ell = 0, \dots, 5$$

$$\tilde{M}_{\ell\pm}(W) = |M_{\ell\pm}(W)|e^{i(\phi_\ell - \phi_0)}, \quad \ell = 1, \dots, 5$$



Reduced multipoles

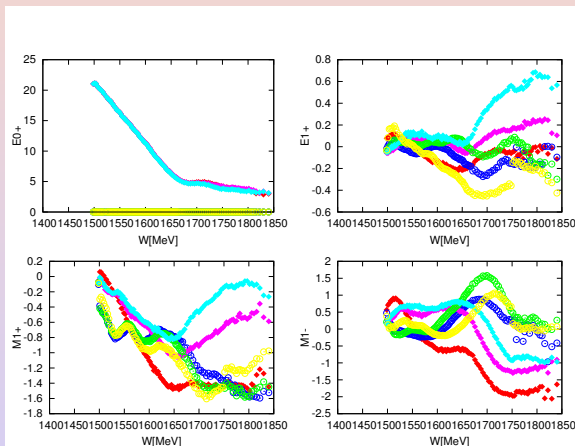


Figure : Red and blue-reduced multipoles obtained using 15a as constraint in FT. Green and magenta-reduced multipoles obtained using 15c as constraint in FT. Cyan and yellow -reduced multipoles obtained using 15d2 as constraint in FT



Reduced multipoles

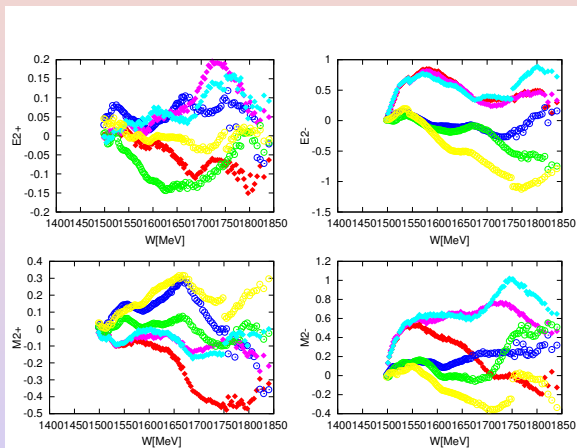


Figure : Red and blue-reduced multipoles obtained using 15a as constraint in FT. Green and magenta-reduced multipoles obtained using 15c as constraint in FT. Cyan and yellow -reduced multipoles obtained using 15d2 as constraint in FT



Reduced multipoles

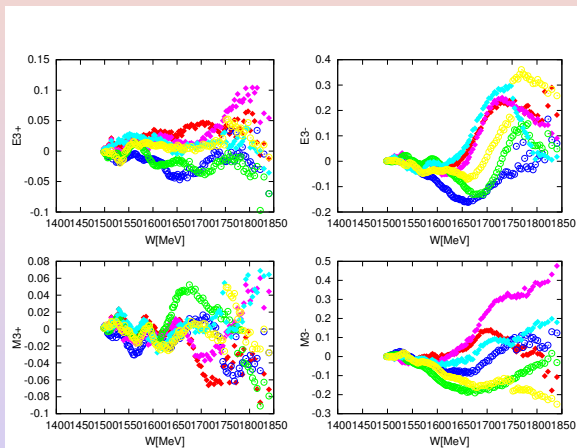


Figure : Red and blue-reduced multipoles obtained using 15a as constraint in FT. Green and magenta-reduced multipoles obtained using 15c as constraint in FT. Cyan and yellow -reduced multipoles obtained using 15d2 as constraint in FT



$$H_1^{a,c,d_2}(x, W) = |H_1^{a,c,d_2}(x, W)| e^{i\phi_1^{a,c,d_2}(x, W)}$$

Reduced helicity amplitudes

$$\tilde{H}_k^{a,c,d_2}(x, W) = |H_k^{a,c,d_2}| e^{i(\phi_k^{a,c,d_2}(x, W) - \phi_1^{a,c,d_2}(x, W))}, \quad k = 1, 2, 3, 4$$



Reduced helicity amplitudes- $W=1487\text{MeV}$

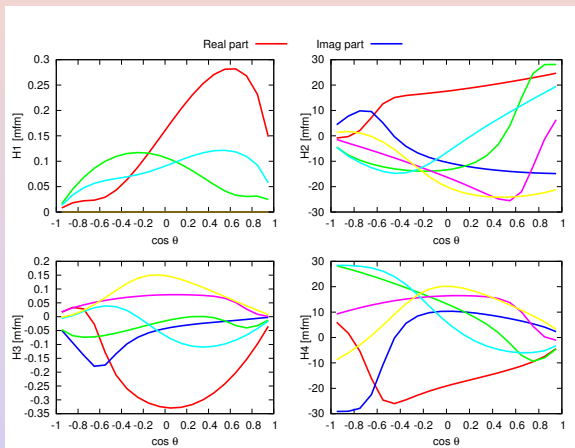


Figure : Red and blue-reduced helicity amplitudes obtained using 15a as constraint in FT. Green and magenta-reduced helicity amplitudes obtained using 15c as constraint in FT. Cyan and yellow-reduced helicity amplitudes obtained using 15d2 as constraint in FT



Reduced helicity amplitudes- $W=1602\text{MeV}$

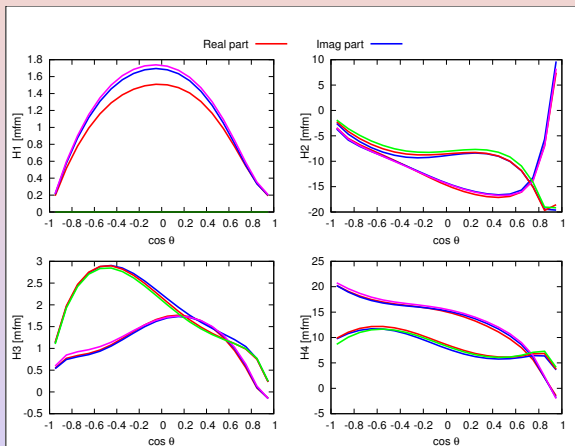


Figure : Red and blue-reduced helicity amplitudes obtained using 15a as constraint in FT. Green and magenta-reduced helicity amplitudes obtained using 15c as constraint in FT. Cyan and yellow -reduced helicity amplitudes obtained using 15d2 as constraint in FT



Reduced helicity amplitudes- $W=1699\text{MeV}$

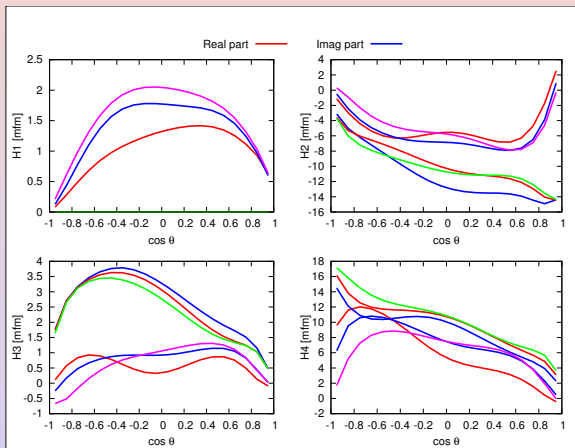


Figure : Red and blue-reduced helicity amplitudes obtained using 15a as constraint in FT. Green and magenta-reduced helicity amplitudes obtained using 15c as constraint in FT. Cyan and yellow-reduced helicity amplitudes obtained using 15d2 as constraint in FT



Reduced helicity amplitudes- $W=1801\text{MeV}$

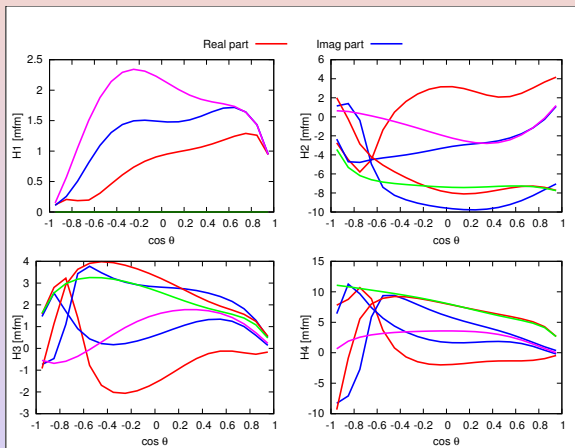


Figure : Red and blue-reduced helicity amplitudes obtained using 15a as constraint in FT. Green and magenta-reduced helicity amplitudes obtained using 15c as constraint in FT. Cyan and yellow -reduced helicity amplitudes obtained using 15d2 as constraint in FT



Reduced helicity amplitudes- $W=1998W$

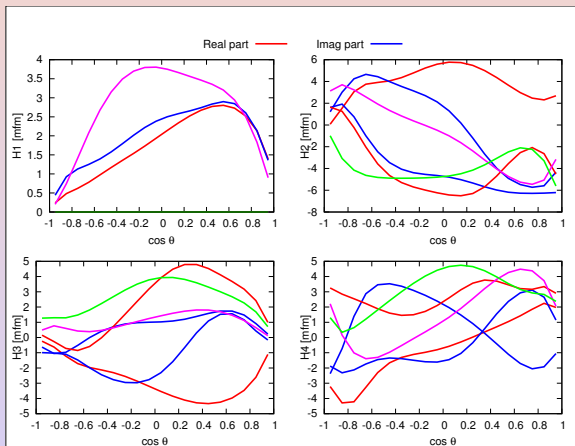


Figure : Red and blue-reduced helicity amplitudes obtained using 15a as constraint in FT. Green and magenta-reduced helicity amplitudes obtained using 15c as constraint in FT. Cyan and yellow-reduced helicity amplitudes obtained using 15d2 as constraint in FT



We present fixed-t fits to the MAID2015a pseudodata. In present calculations 8 observables were fitted: $d\sigma/d\Omega$, $\Sigma d\sigma/d\Omega$, $Td\sigma/d\Omega$, $Fd\sigma/d\Omega$, $Ed\sigma/d\Omega$, $Gd\sigma/d\Omega$, $Hd\sigma/d\Omega$, and $Pd\sigma/d\Omega$.

$$\chi^2 = \chi_{data}^2 + \chi_{FT}^2 + \Phi$$

$$\chi_{FT}^2 = q \sum_{k=1}^4 \sum_{n=1}^{N_{th}} \left[\left(\frac{\text{Re}H_k(\omega, x_n)^{fit} - \text{Re}H_k(\omega, x_n)^{start}}{\varepsilon_{k,n}^{Re}} \right)^2 + \left(\frac{\text{Im}H_k(\omega, x_n)^{fit} - \text{Im}H_k(\omega, x_n)^{start}}{\varepsilon_{k,n}^{Im}} \right)^2 \right]$$

H_k -helicity amplitudes from SE -1st ($-0.075 \text{ GeV}^2 > t > -2.00 \text{ GeV}^2$)

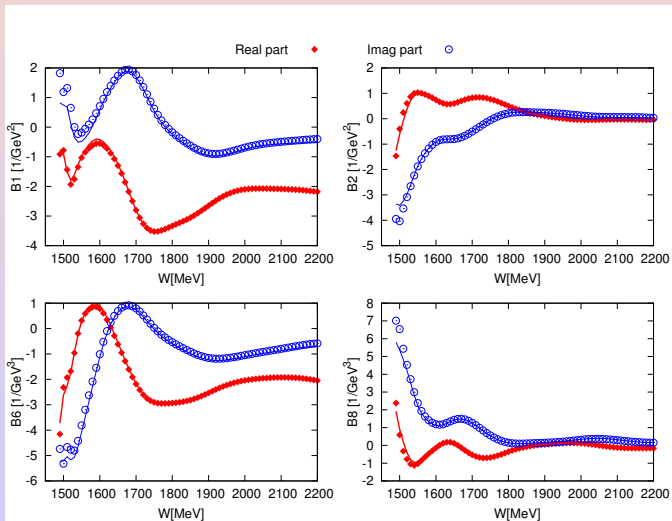
q - adjustable weight factor. ($q = 1$).

$\varepsilon_{k,n}^{Re}$ and $\varepsilon_{k,n}^{Im}$ are errors. In this case $\varepsilon_{k,n}^{Re} = \varepsilon_{k,n}^{Im} = 1$. As a constraint we

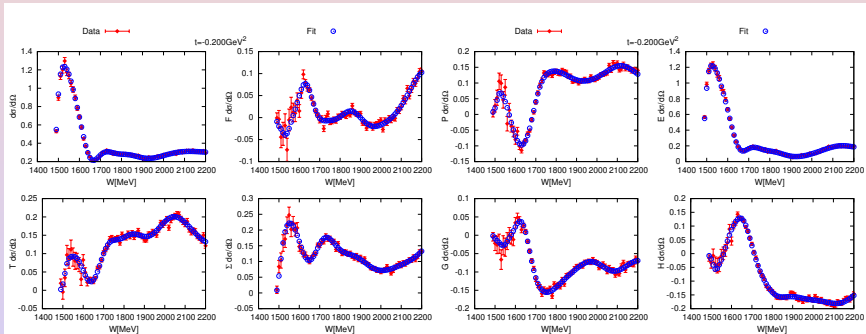
used etaMAID2015b. Red diamonds and blue circles shown etaMAID2015b initial solution. Red and blue solid lines are FT fit of IA.



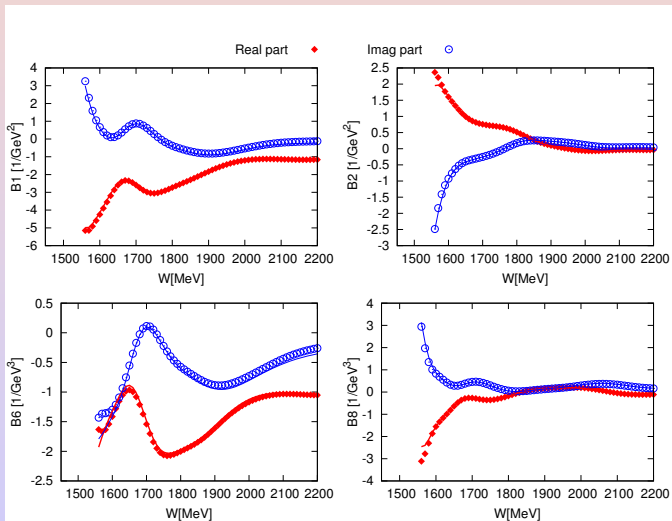
FT invariant amplitudes



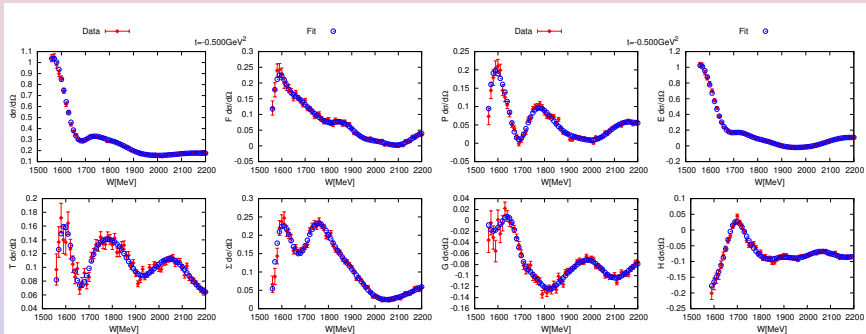
Fit of pseudo data etaMAID2015a



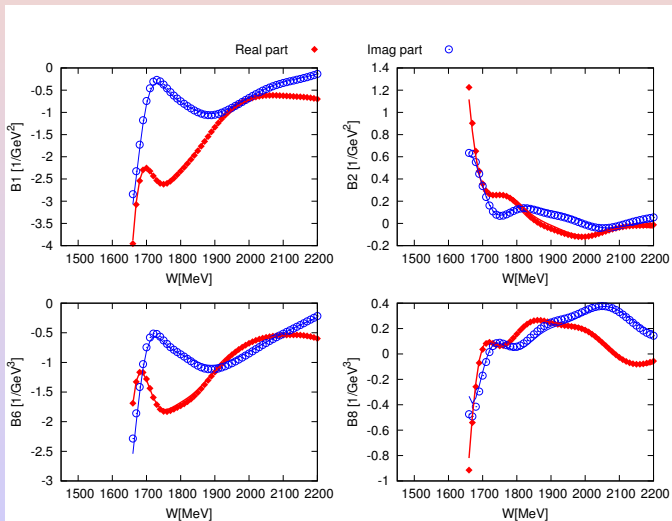
FT invariant amplitudes



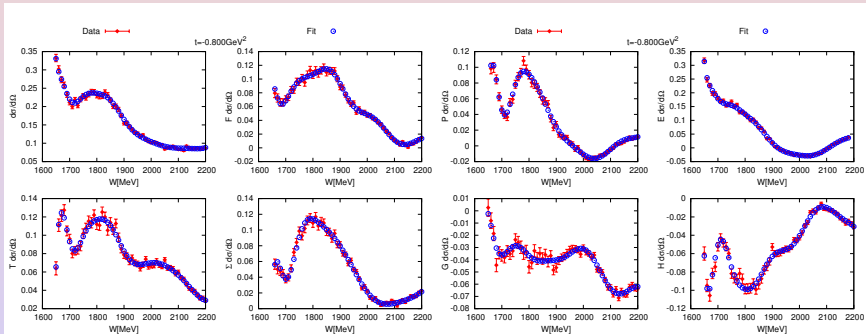
Fit of pseudo data etaMAID2015a



FT invariant amplitudes



Fit of pseudo data etaMAID2015a



We present SE fits to the MAID2015a pseudodata. In present calculations 12 observables were fitted: $d\sigma/d\Omega$, $\Sigma d\sigma/d\Omega$, $Td\sigma/d\Omega$, $Fd\sigma/d\Omega$, $Ed\sigma/d\Omega$, $Gd\sigma/d\Omega$, $Hd\sigma/d\Omega$, and $Pd\sigma/d\Omega$.

Multipoles up to H-waves ($l=5$) were fitted.

$$\chi^2 = \chi_{data}^2 + \chi_{FT}^2 + \Phi_{trunc}$$

H_k -helicity amplitudes from FT ($-0.075\text{GeV}^2 > t > -2.00\text{GeV}^2$). As a constraint we used etaMAID2015b.

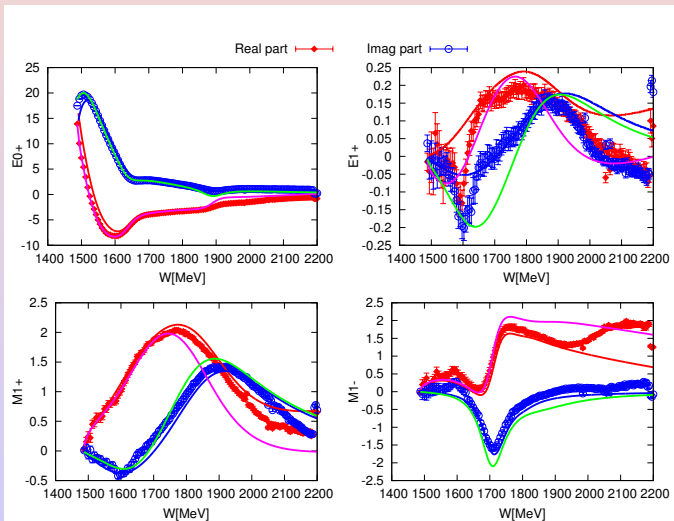
q - adjustable weight factor. ($q = 1$).

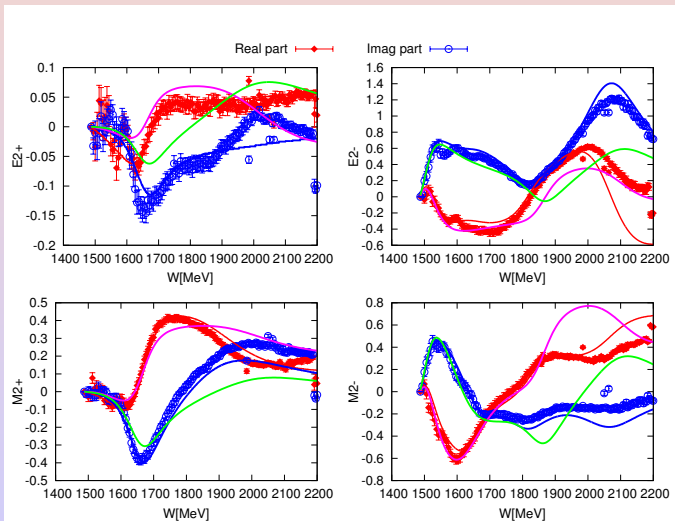
$\varepsilon_{k,n}^{Re}$ and $\varepsilon_{k,n}^{Im}$ are errors. In this case $\varepsilon_{k,n}^{Re} = \varepsilon_{k,n}^{Im} = 1$.

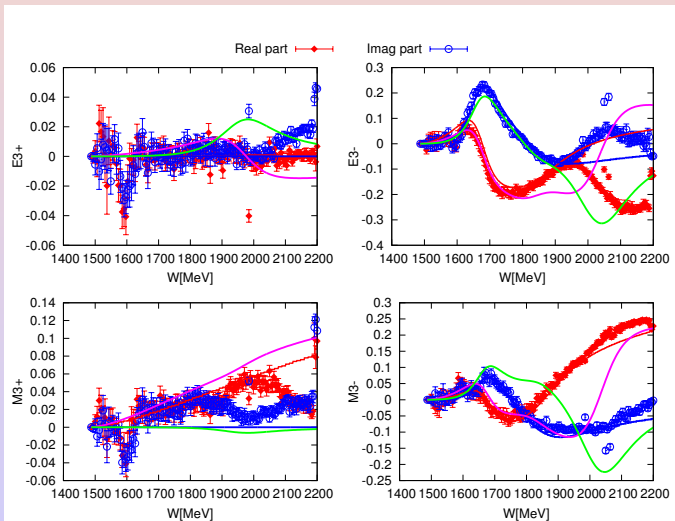
Red and blue solid lines are multipoles from etaMAID2015a.

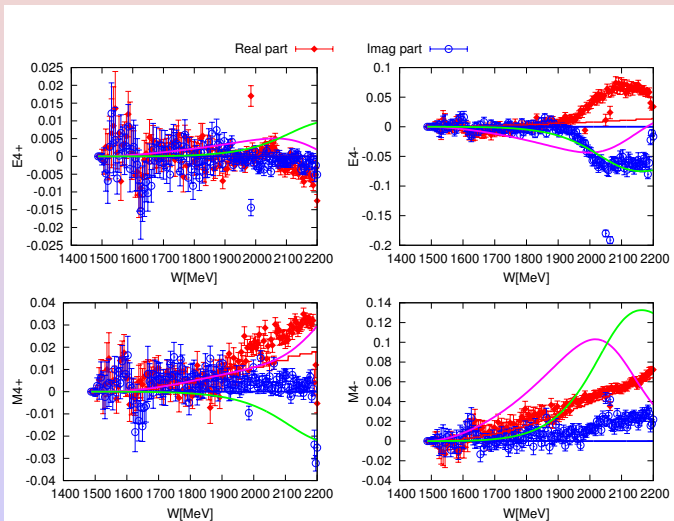
Magenta and green solid lines are multipoles from etaMAID2015b.

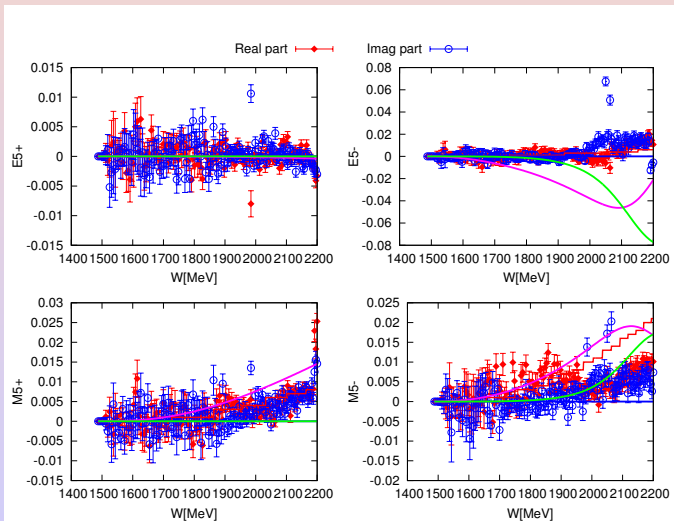


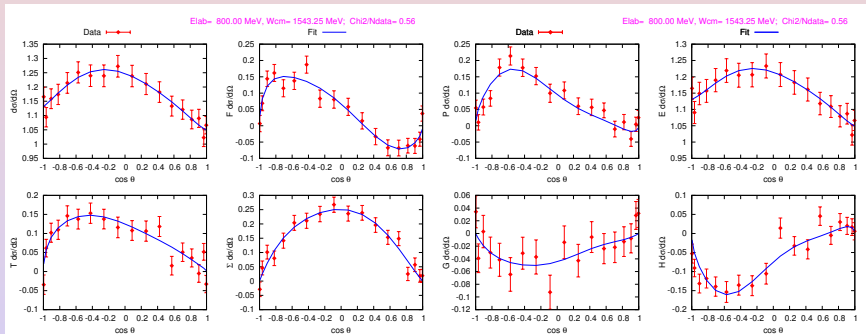


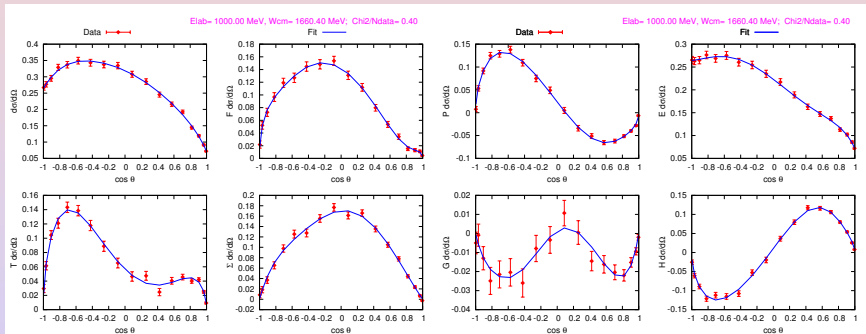


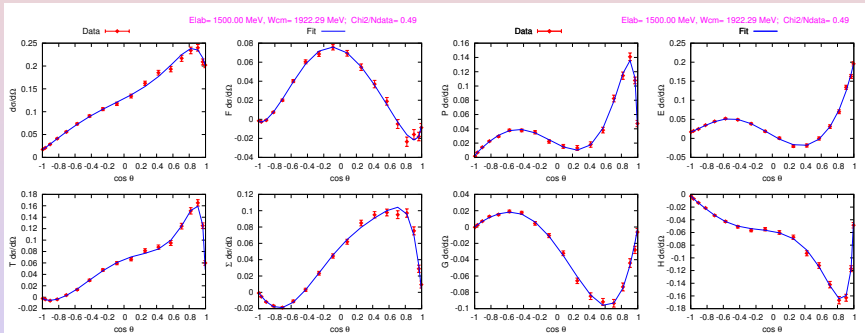




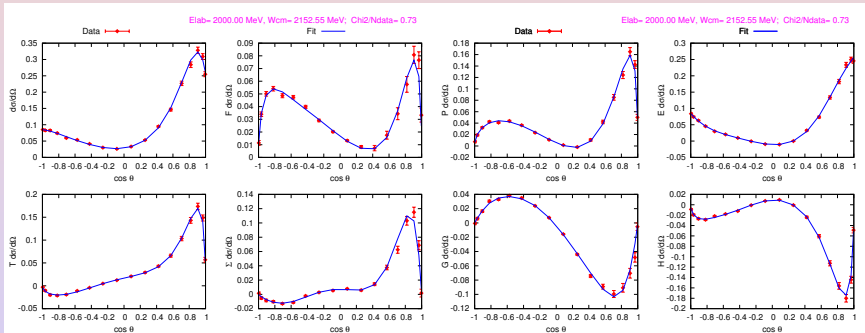




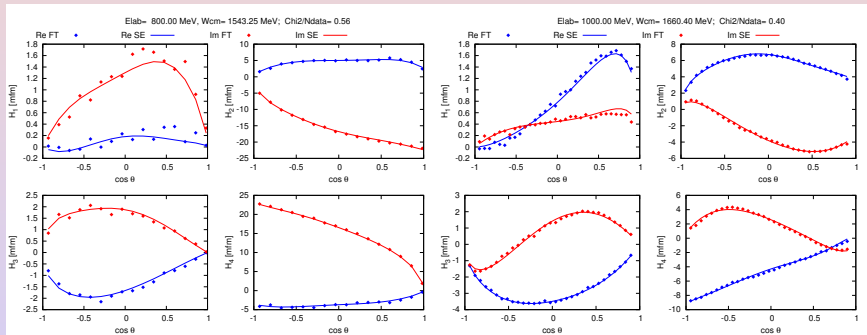




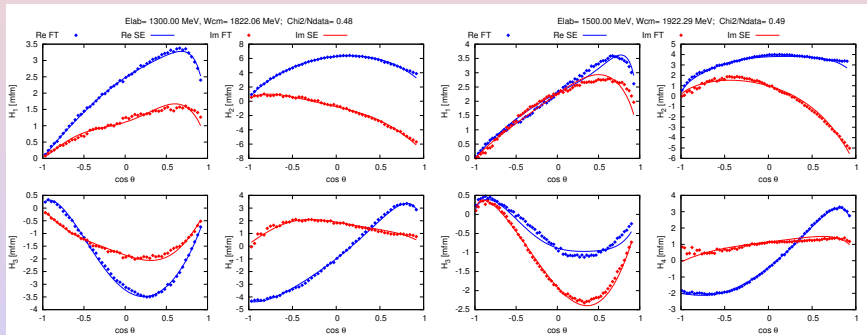
SE PWA pseudo etaMAID2015a



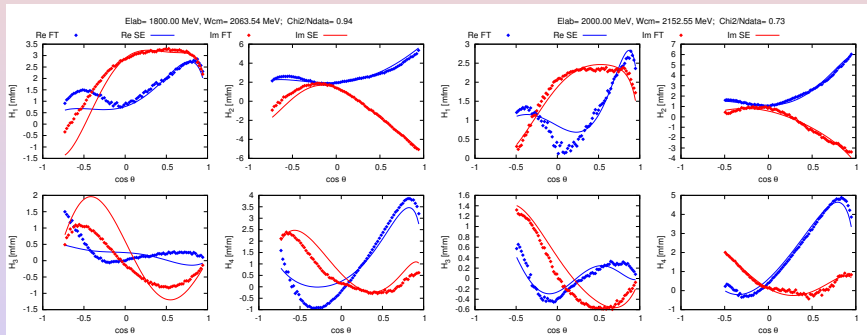
SE PWA pseudo helicity amplitudes



SE PWA pseudo helicity amplitudes

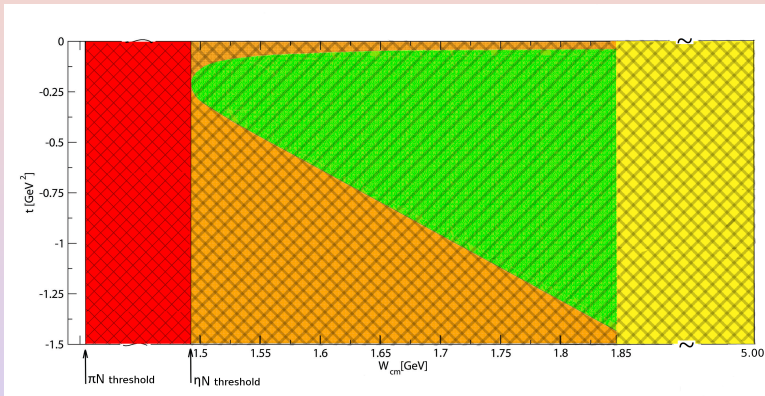


SE PWA pseudo helicity amplitudes



- Applied method of PWA is based only on Mandelstam hypothesis and fixed-t and fixed-s analyticity, and, as such is model independent.
- PWA with constraint from fixed-t amplitude analysis produce multipoles which are consistent with crossing symmetry and fixed-t analyticity.
- Invariant amplitudes (Helicity amplitudes) obtained in fixed-t AA show a good consistency with fixed-s analyticity. It implies that our amplitudes are consistent with both- fixed-t and fixed-s analyticity.
- Weak point and the main problem is strong dependence of our results on constraining solution.

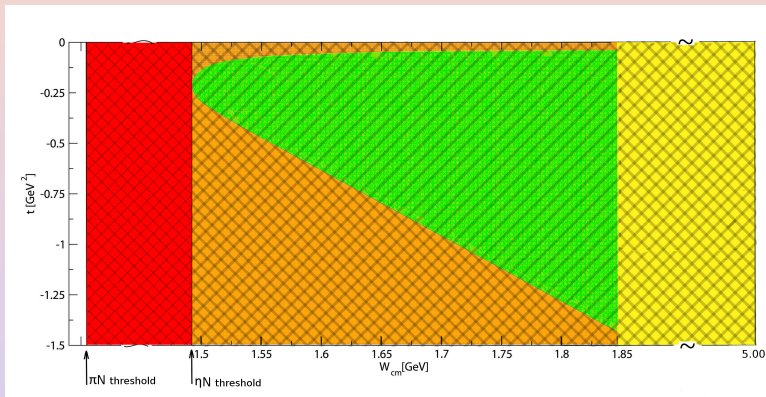




- Include input from “red” region taking results from Aznauryan's work - it will make our analysis (slightly?) model dependent
- Include results on imaginary parts of IA from “orange” region
- Spread constraining PWA solution by randomizing constraining solution changing it randomly (let say 10%)

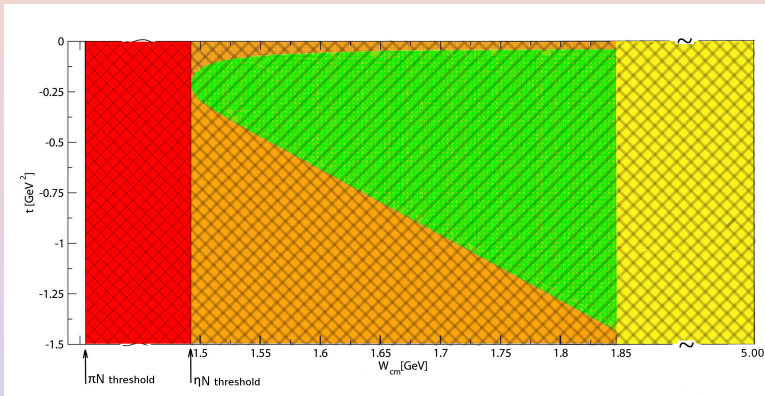


Further research



- Include input from “red” region taking results from Aznauryan's work - it will make our analysis (slightly?) model dependent
- Include results on imaginary parts of IA from “orange” region
- Spread constraining PWA solution by randomizing constraining solution changing it randomly (let say 10%)





- Include input from “red” region taking results from Aznauryan’s work - it will make our analysis (slightly?) model dependent
- Include results on imaginary parts of IA from “orange” region
- Spread constraining PWA solution by randomizing constraining solution changing it randomly (let say 10%).

